

CN 044

This document is made available electronically by the Minnesota Legislative Reference Library as part of an ongoing digital archiving project. <http://www.leg.state.mn.us/lrl/lrl.asp>

METAL COMPOSITION AND SIZE DISTRIBUTION OF ATMOSPHERIC PARTICULATE
MATTER IN REMOTE NORTHEASTER MINNESOTA

APRIL, 1978

File Copy

METAL COMPOSITION AND SIZE DISTRIBUTION OF ATMOSPHERIC PARTICULATE
MATTER IN REMOTE NORTHEASTERN MINNESOTA

by

S. J. Eisenreich
S. A. Langevin
J. D. Thornton

Environmental Engineering Program
Department of Civil and Mineral Engineering
University of Minnesota
Minneapolis, Minnesota 55455

Prepared for

Minnesota Environmental Quality Council

April, 1978

TABLE OF CONTENTS

i

page

Conclusion	
List of Tables	
List of Figures	
Introduction	
Literature Review	
Experimental	
Sampling Equipment	
Sampling Procedure	
Sampling Location	
Metal Analysis of Cascade Impactor Stages	
Results and Discussion	
Introduction	
Observations on Particle Appearance	
Reproducibility of Sampling and Analysis	
Metal Size Distributions	
Elemental Enrichment Factors	
Calculation of Mass Median Diameters	
Temporal Variations in Metal Particle Size	
Dry Deposition Rates	
References	
Appendix A. Cascade Impactor Particle Size Data	A-1
Appendix B. Mass Median Diameter Calculation	B-1
Appendix C. Calculation of Loading Rates Due to Dry Deposition	C-1

CONCLUSIONS

ii

1. Trace metal content of air particulates in NE Minnesota was low, and typical of remote continental aerosol.
2. Major metal content (Fe, Al, Mn) of air particulates in NE Minnesota was low but was influenced by iron taconite mining and processing, power generation facilities and vehicular traffic on dirt roads.
3. Metal concentrations in air particulates were higher at Hoyt Lakes than at Kawishiwi.
4. Copper and nickel concentrations were below detection limits during nearly all sampling events.
5. The size of Fe, Al, Mn and Ca in air particulates generally decreased with decreasing particle size.
6. The size of Pb in air particulates increased with decreasing particle size typical of gasoline combustion.
7. Average mass median diameters at Kawishiwi were Fe, 6.9 μm ; Al, 4.9 μm ; Ca, 7.8 μm ; Mn, 5.2 μm , Pb, 1.1 μm .
8. Average mass median diameters at Hoyt Lakes were Fe, 7.3 μm ; Al, 4.5 μm ; Ca, 5.2 μm ; Mn, 5.0 μm ; Pb, 0.9 μm .
9. Dry deposition rates based on metal size distributions were typical of remote continental areas, except for Fe.
10. Seasonal variations in Fe enrichment factors at both sites suggest that taconite iron mining and associated activities may be the major contributor to the suspended particulate load in the atmosphere of the region.

1. Mass median diameter of selected metals.
2. Samplers for collecting size differentiated air particulates.
3. Particle size cutoff of cascade impactor stages.
4. Recovery studies of metals in standard orchard leaves.
5. Instrumental conditions for cascade impactor metal analysis.
6. Metal composition of nuclepore filter blanks.
7. Variation in metal size distribution from cascade impactors operated simultaneously.
8. Total metal in cascade impactor samples.
9. Comparison of mean total metal concentrations from cascade impactor and membrane filter analysis of atmospheric particulates.
10. Mean atmospheric metal concentrations in different size fractions at Kawishiwi Laboratory.
11. Mean atmospheric metal concentrations in different size fractions at Hoyt Lakes.
12. Atmospheric metal size distribution at Kawishiwi Lab.
13. Elemental composition of earth's crust.
14. Metal enrichment factors at Kawishiwi Lab and Hoyt Lakes.
15. Mass median diameters of particulates in N.E. Minnesota.
16. Atmospheric loading of trace metals in northeastern Minnesota.
17. Comparison of dry deposition estimates for atmospheric particulates.

LIST OF FIGURES

iv

Title	page
1. Trimodal distribution of typical atmospheric aerosol illustrating dominant removal mechanisms.	
2. Mass median diameter and dry deposition velocity at Chilton (July-Dec. 1973).	
3. Cascade impactor sampling locations.	
4. Size distributions of Fe, Al, Ca, Mn, and Pb in north-eastern Minnesota aerosol.	
5. Metal particle size distribution in late summer, 1976.	
6. Metal particle size distribution in spring, 1977.	
7. Crustal enrichment factor for Fe as a function of particle size and time.	
8. Log mmd (Fe and Pb) at Kawishiwi Lab and Hoyt Lakes as a function of time.	
9. Iron, Al, and Pb concentrations greater than and less than 2 μm diameter as a function of time at Kawishiwi Lab.	
10. Iron, Al, and Pb concentration greater than and less than 2 μm diameter as a function of time at Hoyt Lakes.	
c-1. Deposition velocity to a water surface (particle density of 1.5 g/cm^3)	

INTRODUCTION

v

Mineral mining has been an important facet of the economy and life-style in northeastern Minnesota for many years. The taconite iron industry represents the largest single source of iron for the production of steel in the U.S. Along the eastern ridge of the Mesabi Iron Range lies the surface contact zone of the Duluth Gabbro which contains significant copper and nickel mineralization in the form of sulfides. The Duluth Gabbro Complex is a large body of mafic and anorthositic plutonic rocks of late Precambrian age that underly nearly 2500 square miles of northeastern Minnesota. Copper-nickel mining may become a reality within the next five years due to the presence of ~ 890 billion of recoverable base metal sulfides. Prior to initiation of site-specific environmental impact statements (EIS), the State of Minnesota through the Environmental Quality Council authorized the preparation of a regional environmental impact statement. One objective of the EIS was to obtain baseline data on the air quality of the region. The work described here details the size distribution of selected metals in atmospheric particulates as related to seasonal and geographical variations and dry deposition.

LITERATURE REVIEW

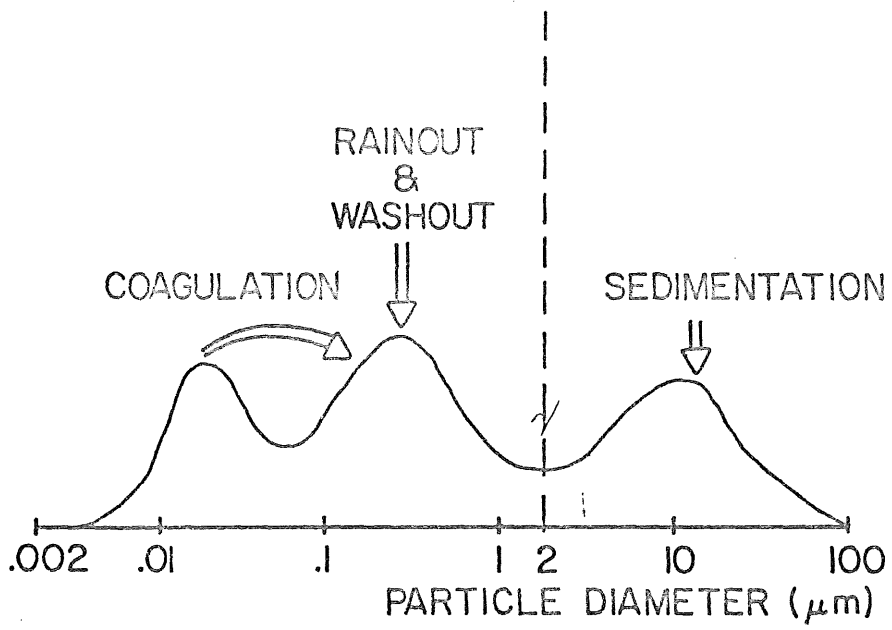
The majority of atmospheric particulate matter is lognormally distributed with respect to size. In a survey of 329 distributions, Blifford and Gillette (1971) found 98% to be lognormally distributed. These investigators also found that the elements Cl, S, K, Ca, Si, and Ti were generally lognormally distributed in aerosols collected at various altitudes over remote sections of Nebraska, California, and the Pacific Ocean. Whitby (1977) has identified 3 modes (each lognormally distributed) in aerosol populations, illustrated in Figure 1. The nuclei mode (.015 - .04 μm diam.) is formed by hot vapor condensation of combustion products, and the particles are not subject to sedimentation due to small sizes. The accumulation mode (.15 - .5 μm dia.) is formed by condensation growth and coagulation of particles in the nuclei mode. Removal from the atmosphere is predominantly by rainout and washout mechanisms. The coarse particle mode (5 - 30 μm dia.) is derived from wind-blown dust, poorly controlled emissions, sea spray, volcanic activity, and plant debris. The primary removal mechanism is sedimentation. There is very little interaction between the coarse particle mode and the two submicron modes. The relative contribution from each of these modes to the total aerosol population is dependent on the aerosol source and age.

Measurements of size distribution of atmospheric particulates have been made by numerous researchers. Methods of sampling and type of sampler used are largely dependent on the overall objectives of each study. Size distributions have been examined with respect to number, surface area, and volume (Sverdrup et al. 1975), altitude (Blifford and Gillette, 1972), time (Graedel and Franz, 1974), mass (Lee and Goranson, 1972), and chemical composition (Lee et al. 1972; Flocchini et al. 1976). Chemical composition

is of particular interest since aerosols from a given source often have characteristic size distributions for individual elements or compounds (Hardy et al. 1976; Martens et al. 1973; Dzubay and Stevens, 1975; Pacinga et al. 1975). The majority of the chemical analysis on size differentiated aerosol has emphasized metallic elements, although some anionic constituents, such as Br (Pacinga et al. 1975), Cl (Martens, 1973), and SO_4 (Kadowaki, 1976) have been determined. Bromine is important as a tracer of aerosols derived from leaded gasoline, while Cl is a major component of sea salt aerosols.

Studies undertaken thus far have concentrated on urban, marine, and remote environments, with urban sites being by far the most thoroughly investigated. For example, Gladney et al. (1974) collected aerosols at the Massachusetts Institute of Technology (MIT) and a residential area in Massachusetts. Total concentrations were comparable for the two sites for Al, Fe, and Mn. Vanadium and Zn were 10 and 3.5 times as high respectively at the MIT site. Vanadium was found primarily in small particles, but also showed a peak occurring between 4 and 8 μm . The V concentrations have decreased in recent years however, due to lower V concentrations in residual oil used for heating (Faoro and McMullen, 1977). In addition to V, Gladney et al. (1974) found Zn, Se, and Sb to be associated with small particles. Aluminum, Sc, Fe, and Th were found on large particles, and were partly attributed to fly ash from a coal combustion source. The Al and Fe distributions were distinctly different however, with Al concentrations dropping off more sharply than Fe for small particles. A theory offered by Gladney et al. (1974) is that Fe, being in the form of sulfides, may be partially vaporized and then condensed on to small particles. Cobalt, Mn, and Ce showed a mixed size distribution. Nifong et al. (1972), in a study of 29 elements in size differentiated

Figure 1.
Trimodal distribution of typical atmospheric aerosol illustrating
dominant removal mechanisms. (From Whitby, 1977)



| Aitken nuclei |----->| Accumulation mode |----->| Sedimentation mode |

| Fine particles |----->| Coarse particles |

aerosols from the Chicago-Gary, Indiana area, concluded that Si, Ca, and Mg were from natural sources; Pb, Mn, and Zn were from anthropogenic sources; and Fe and Al were contributed from both natural and man-induced processes. Iron, Mn, Cr, Co, Sc, Th, Ca, Mg, and Ti were primarily found on particles $> 10 \mu\text{m}$. Similar results were found by Pacinga and Jervis (1976) in urban and industrial aerosols from Toronto. Aluminum, Ca, Co, La, Mg, Fe, Sn, Sc, Na, and Ti were all well correlated with each other and had low enrichment factors (EF). These elements were attributed to a soil source. Vanadium, Mn, Zn, and Pb were all significantly enriched and associated with smaller particles. Mass median diameters (MMD's) (see Appendix B) were computed and are listed in Table 1 for comparison. Hardy et al. (1976), in an attempt at source identification, examined 13 elements in Miami aerosols. The bulk of the study dealt with the comparison of elemental ratios in different size fractions with corresponding ratios for the earth's crust, auto exhaust, and sea water.

The impact of gasoline combustion on the quality of urban air has been of recent interest. Pacinga et al. (1975) used Br/Pb ratios in size differentiated aerosols collected near roadways and lead refineries in Toronto to estimate the relative contribution of lead from each of these two sources. The method used is based on the well documented belief that Br in urban air is due almost exclusively to gasoline combustion. Close to roadsides Pb particles were predominately submicron in size, compared to those near refineries which were predominately greater than $3 \mu\text{m}$. In a similar investigation, Martens et al. (1973) examined Pb and Br in San Francisco Bay area aerosol and found little variation in the concentrations of the two elements in size ranges above $0.4 \mu\text{m}$; however, there was a dramatic increase in concentration less than $0.4 \mu\text{m}$. Numerous similar studies of urban areas are reported in the literature (Huntzicker et al. 1975; Miller et al. 1976; Whitby et al. 1975).

In an extensive two part study by Lee and Goranson (1975) and Lee et al. (1975), size differentiated air particulates were collected and characterized from six major U.S. cities including Denver, Chicago, Washington, D.C., Cincinnati, St. Louis, and Philadelphia. The first study looked at the size distribution of total suspended particulates. Average MMD's from one year of sampling varied from 0.4 μm in Denver to 0.83 μm in St. Louis. The average geometric standard deviations (σ_g) for the distributions were also presented. The σ_g value for a distribution is a measure of the dispersion or spread of the aerosol population about the mean. For example, a σ_g equal to 1.0 would be indicative of a perfectly monodisperse aerosol. In this study, σ_g varied from 5.22 for Washington, D.C. to 10.5 for Denver. The second part of the study applied similar statistical treatments to selected trace metals. For the six cities, the ranges of MMD's for selected metals are listed in Table 1. These results are consistent with others already discussed with the exception of Fe (MMD = 2.34 - 3.15), which is usually found on particles greater than $\sim 5 \mu\text{m}$. However, the association of Fe with smaller particles is consistent with Lundgren's 2.2 μm MMD for Fe in samples collected at Riverside, California (1971). In 8 of 10 samples collected, the back-up filter (dia. $< .5 \mu\text{m}$) contained more Fe than each of the preceding stages.

In another study, conducted by Dzubay and Stevens (1975), in St. Louis, it was observed that particles less than 2 μm in diameter were black in color, whereas particles greater than 2 μm were light tan. These investigators also found 75% of Zn, S, Br, and Pb in the particle size range less than 2 μm , in contrast to Fe, Si, Ca, and Ti, 75% of which were found on particles greater than 2 μm .

An important application of aerosol size distribution data is in the assessment of atmospheric inputs of pollutants to natural water bodies.

TABLE 1

Mass Median Diameter of Selected Metals (μm)

Metal	Toronto ¹	Several Major U.S. Cities ²	Chilton England(remote) ³	Lake Michigan ⁴
Fe	6	2.34 - 3.15	2.5	4.3 - 6.3
Al	8		4.4	5.8 - 8.1
Ca	7			7.7 - 10.2
Mn	2.4		1.3	
Zn	1.2	1.03 - 1.29	.86	
V	.9		.64	
Pb	.7	.42 - .69	.56	1.2 - 3.4
Ni	1.2	1.05 - 1.52		
Mg	7			6.2 - 10.0
Na	4		3.1	
Cu		1.07 - 1.59		1.5 - 4.7
Cr			1.0	1.8 - 3.3

¹ Pacinga and Jervis (1976)

² Lee et al. (1975)

³ Cawse (1974)

⁴ Schmidt (1977)

Edgington and Robbins (1976) indirectly measured the atmospheric input of Pb to Lake Michigan from urban air pollution plumes by examining the recent sedimentary records of the lake. In a more direct study, Schmidt (1977) calculated dry and wet loadings of several trace metals by relating deposition velocities to MMD's. Schmidt calculated MMD's from size differentiated aerosols collected directly over Lake Michigan (Table 1).

Remote areas have not been evaluated as extensively as urban areas for aerosol size data. Of the work that has been done, perhaps the most thorough is a survey done by Cawse (1974) in the United Kingdom. Seven non-urban sites were monitored for elemental composition of particulates, rainfall, dry deposition, and size differentiated air particulates (2 of the 7 sites). Cawse calculated deposition velocities, enrichment factors (with Sc as a soil reference), and MMD's. Generally, V, Zn, As, Se, Br, Sb, Cs, and Pb had MMD's $<1 \mu\text{m}$; Cr, Mn, Fe, and Co had MMD's from 1-3 μm ; and Na, Al, Sc, and Ce had MMD's $>3 \mu\text{m}$. Table 1 compares some of the actual numbers from one site with other works. Deposition velocities arrived at from dry deposition rates were shown to correlate well with MMD's as seen in Figure 2.

Blifford and Gillette (1972) collected air samples with a 3 stage high volume impactor at various altitudes over the Pacific Ocean and Death Valley, California. Chloride and Si were used as tracers of sea and land derived particulates, respectively. No significant conclusions were drawn from the minimal amount of metal analysis performed in this study. Sverdrup et al. (1975) monitored air over the Mojave Desert and found Zn and Pb concentrations typically on the order of 10 and 50 ng/m^3 , respectively. The Pb concentration exceeded 700 ng/m^3 on one occasion. Metals were not monitored with respect to

Figure 2.
Mass median diameter and dry deposition velocity at Chilton (July-Dec.
1973). (From Cawse, 1974).

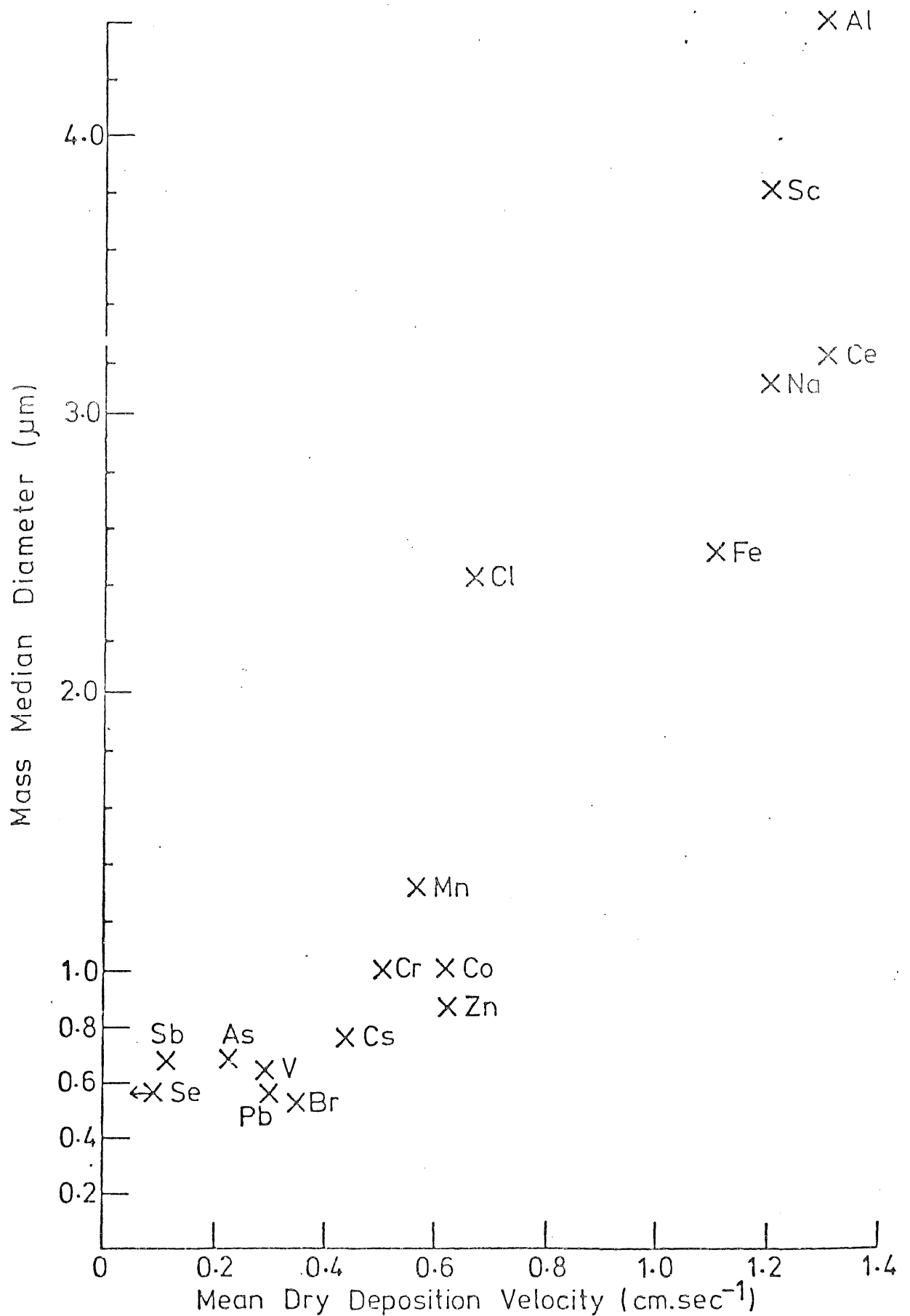


Figure 2. MASS MEDIAN DIAMETER AND DRY DEPOSITION VELOCITY AT CHILTON (JULY-DEC. 1973)

(From Cawse, 1974)

size; however, total particulates usually contained a significant mass fraction below 1 μm diameter. Aerosol from north Florida were collected for elemental analysis in 6 size ranges by Johansson et al. (1976) to evaluate a remote background environment. Total Fe and Pb concentrations were on the order of 150 and 30 ng/m^3 , respectively. In addition, K, Ca, Ti, and Fe were found in large particle size ranges; and S, Pb, and Br were found in small particle size ranges. Zinc had relatively equal concentrations in all size ranges. A unique sampling technique was utilized over the world's oceans to assess the soil derived component of marine air (Chester et al. 1974). Particles were collected by suspending a 1 m^2 nylon mesh above the bow of a ship. The sampling technique was found to be relatively selective for particles $> 4\mu\text{m}$ (usually derived from soil). Using Fe to calculate EF's, Mn, Ni, Co, Ca, Cr, V, Ba, and Sr were found not to be enriched; Sn, Pb, and Zn were enriched. Concentrations were highly variable but generally lower than remote land areas.

Based on the limited amount of information available, remote areas appear to have similar size distributions as urban areas for the corresponding metals. The primary difference is in total concentration, with urban areas generally five to ten times as high for most metals. There are of course exceptions to the rule. Enrichment factors are also smaller in remote areas, although some elements appear to be enriched in all types of environments, e.g. Pb and Zn.

A multitude of devices is available for sampling aerosols with respect to size. Table 2 lists some of the samplers that have been used by different researchers (references in table are not necessarily the developer of the instrument). The majority of the samplers operate on the basis of inertial impaction. The cascade impactor removes particles by causing them to leave

TABLE 2

Samplers For Collecting Size Differentiated Air Particulates

Sampler	Size Range (μm)	No. Stages	Flow Rate (ℓ/min)	Reference
Anderson Hi-Vol Impactor	<1.1 - > 7.0	4 + B.F.*	570	Pacinga and Jervis (1976)
Modified Anderson Impactor	< .6 - >3.2	5 + B.F.	150	Lee et al. (1972)
Anderson Impactor	< .4 - >9.2	7 + B.F.	29	Martens et al. (1976)
Lundgren Multiday Impactor	< .5 - >16	4 + B.F.	15-150	Lundgren (1971)
Delron Cascade Impactor DCI-5	< .25 - > 4	5 + B.F.	1.0	Hardy et al. (1976)
Delron Cascade Impactor DCI-6	< .5 - >16	6 + B.F.	12.5	This Study
Electrical Aerosol Analyzer	.01 - 1.0	-	-	Miller et al. (1976)
Scientific Advances Co. Cascade Impactor	<.5 - >16	6 + B.F.	12.5	Gladney et al. (1976)
Goetz Aerosol Analyzer				Ludwig and Robinson (1968)
Environmental Research Corporation Dichotomous Sampler	<2 >2	2	49	Dzubay and Stevens (1975)
Climet Instruments Optical Particle Counter	.3 -> 3.0	6	-	Graedel and Franey (1974)

* B.F. - Back-up Filter

the fluid streamlines and impact on a surface. Increasing the air velocity sequentially with each stage by decreasing the diameter of the flow orifice between stage allows collection of particles of smaller diameters in each subsequent stage. The material not collected by impaction is usually collected on an in-line back-up filter placed after the last impaction stage. For a detailed discussion of the theory of inertial impactors, the reader is referred to Marple and Willeke (1976) and Marple and Liu (1974).

The optical particle counter and the electrical aerosol analyzer are for in situ determination of particle number concentrations and are not suited for aerosol collection with subsequent chemical analysis. The primary advantage of the optical particle counter is real time resolution. Changes in particle concentration with time can be resolved down to 10.8 seconds (Graedel and Franey, 1974). The Lundgren impactor can also be used to monitor changes in aerosol populations with time, with the added advantage of subsequent chemical analysis. The time resolution is on the order of hours instead of seconds, and will depend ultimately on the aerosol concentration being sampled and the sensitivity of the post-sampling analytical procedures.

The dichotomous sampler operates on the theory of virtual impaction. The air stream is split into two fractions which are then drawn through filters to remove particles. The larger particles will be removed in one stream, and the smaller particles, the other. The particle cut-off size can be controlled by adjusting the amount of flow going to each stream. The advantages of the dichotomous sampler are the large mass of sample collected for weight determinations and chemical analysis and the elimination of particle bound errors.

When several size fractions are desired for chemical analysis, the sampler of choice is the cascade impactor. Problems do exist with these

impactors, and care should be taken to minimize them. Common problems include wall losses, inlet losses, end effects, changes in cut-off diameter due to changes in flow, and particle bounce-off. Wall losses are due to impaction or diffusion of particles to the walls between stages. Proper design and cleaning of stages can minimize these effects. Inlet losses are a function of inlet design and are largely caused by non-isokinetic sampling. Little has been done to accomplish complete isokinetic sampling, although Davidson (1977) has looked into the problem and made some attempts at semi-isokinetic sampling. End effects are encountered in impactors with rectangular slits; the flow at the ends of the slits is different than the flow along the length of the slit, thus collection efficiency may be diminished. This problem is completely eliminated in round jet impactors, such as the Delron and may be minimized in rectangular slits by increasing the length of the slit. Changes in flow, caused mainly by loading of the back-up filter, will change the effective cut-off diameter of each stage. Corrections can be made if the flow is carefully monitored, but the simplest solution is to use an impactor with a critical flow orifice such as the Delron. The critical flow orifice keeps the flow constant provided the pressure (maintained by a vacuum pump) is not less than a pre-determined minimum value. Particle bounce errors have been investigated and are generally a function of the impaction substrate. If particles bounce or are blown off stages after impaction, they will be collected on a subsequent stage or on the back-up filter, causing an error biased toward smaller particles. Lundgren (1967) found that quantitative collection could only be expected if the impaction surface was coated with a high vacuum silicone grease or similar substance. Dzubay et al. (1976) compared various coated and un-coated surfaces with 2 identical impactors running side by side. Generally, MMD's were smaller when calculated from runs with uncoated surfaces than those with coated surfaces.

Finally, choice of back-up filter is of considerable importance. A filter that has low background contamination is absolutely essential if chemical analyses are to be performed. If weight determinations are to be made, the filter should be stable with respect to mass and preferably non-hygroscopic. Lastly, efficiency of collection for small particles should be high if quantitative results are to be expected. Most filters have their minimum collection efficiency at approximately 0.3 μm diameter, which is in the middle of the size range of the particles to be collected by the back-up filter. A study of particle collection efficiencies for various membrane filters by Liu and Lee (1976) indicated that 0.5 μm and 1.0 μm pore-size Teflon filters were essentially 100% efficient. Nuclepore filters of 0.6 μm pore-size were also acceptable, with greater than 80% efficiency at a pressure drop of 1 cm Hg. Investigators have used many types of filters as back-up including Teflon (Lundgren, 1971), Nuclepore (Hardy et al. 1976), Whatman 41 (Pacinga and Jervis, 1976), and polystyrene (Blifford and Gillette, 1972).

EXPERIMENTAL

Sampling Equipment

Size differentiation of atmospheric particulates was accomplished using a Delron Cascade Impactor Model DCI-6. The impactor is a critical orifice, round, single-jet impactor of the Battelle design (Mitchell and Pilcher, 1959) consisting of six stages and an in-line back-up filter. Particle size cut-offs given in Table 3 are 16, 8, 4, 2, 1, and 0.5 μm equivalent aerodynamic diameters for stages 1 through 6, respectively. The back-up filter collects particles passing the first six stages and less than 0.5 μm diameter. The particle size values represent 50% cut-offs for spherical particles of unit density. Deviation from spherical shape and unit density influences behavior somewhat since aerodynamic particle diameter determines stage collection. Air is drawn through the Delron at a flow rate of ~ 12.5 l/min by maintaining a critical pressure of greater than 17 inches of Hg with a Gast vacuum pump. Flow and cut-off diameter calibrations were performed by the manufacturer and are maintained by critical flow orifice construction.

The impactor is equipped with 37 mm glass slides as the impaction surface mounted downstream of each stage orifice. However, particle bounce-off from hard, flat surfaces can affect particle size distribution. Various types of vacuum or chromatographic greases have been applied to impaction surfaces to minimize particle bounce-off, including paraffin and silicone grease. Apiezon L high vacuum grease has been shown to reduce bounce-off of soil-derived aerosols to less than 0.5% (Flocchini et al. 1976). For this reason, 37 mm diameter, 0.6 μm pore-size Nuclepore filters coated with Apiezon L grease placed on the glass slides were used as impaction surfaces in this study. The Nuclepore filters were coated by carefully dipping each filter held by a teflon-coated forceps into 2% Apiezon L in cyclohexane for a period of 5 seconds. Excess

TABLE 3

PARTICLE SIZE CUTOFF OF CASCADE IMPACTOR STAGES

(DELRON DCI-6)

Stage	Particle Diameter (microns)
1	16.0
2	8.0
3	4.0
4	2.0
5	1.0
6	0.5
B	<0.5

solution was removed by contacting the edge of the filter with clean Whatman 41 filter paper. The Nuclepore filter was then placed on the glass slide, and the cyclohexane allowed to evaporate with the slide and filter in a loosely-covered 50 mm polycarbonate petri dish. After 2 minutes drying time, the filter was sealed tightly in the petri dish with a lid and stored for later use. This procedure minimizes contamination and also results in the filter adhering to the glass slide. Loading of Apiezon L on the filters averaged 0.103 mg/m^2 . Back-up filters were $0.6 \text{ }\mu\text{m}$ pore size Nuclepore filters. The face velocity on the back-up filter during sampling was 3.27 m/sec . Based on work by Liu and Lee (1976), the minimum collection efficiency at this velocity is expected to be greater than 80% for the $0.6 \text{ }\mu\text{m}$ Nuclepore filter.

Sampling Procedure

Delron cascade impactors were transported to the field in sealed, wooden carrying cases with each impactor stage set in place previously in the laboratory. At the sampling site, the impactor was placed on a 48 cm high wooden platform which stabilizes the collector to wind disturbances and provides protection for the pump used. All sampling subsequent to 1 February, 1977, was with cascade impactors covered with an aluminum cone-shaped shield $\sim 28 \text{ cm}$ in diameter to protect the collector inlet from rain, snow, and fallout of large debris. Prior to this date, several samples were contaminated due to light rain or snowfall. The circular cones were constructed in a manner that did not cause alteration of airflow and stage collection properties. Vacuum pump exhaust was directed away and downwind from the cascade impactor with a 1.5 m length of vacuum tubing. Sampling times varied from ~ 15 hours to a maximum of 108 hours. At the end of each sampling event, the impactor was replaced in the wooden carrying case and

transported to the laboratory where collection stages were removed to petri dishes. Loss of particles from coated stages due to shock during transport is unlikely due to the adhesive properties of the grease layer. In the worst case, large particle loss should be no greater than 5% (Flocchini et al. 1976).

Sampling Location

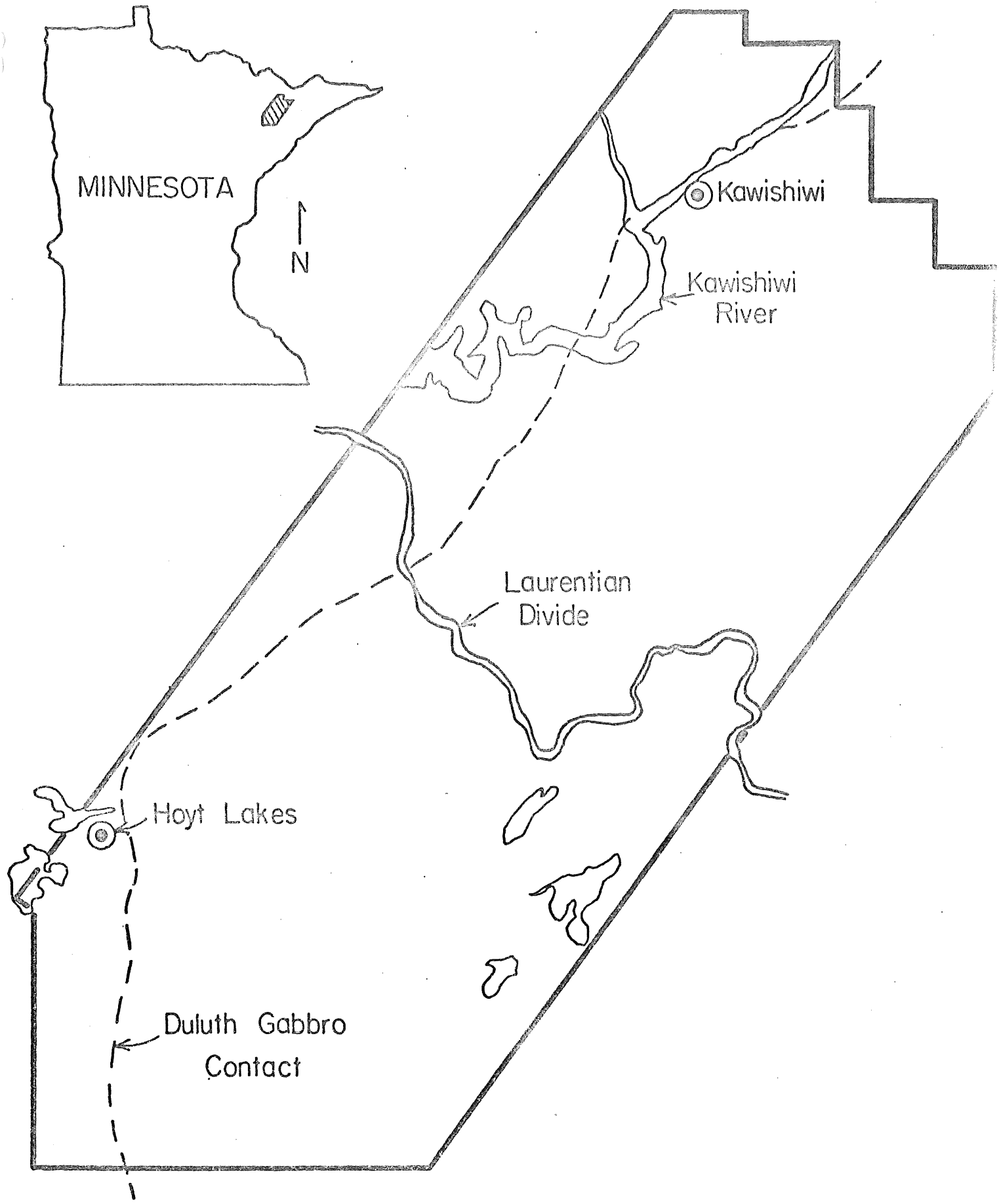
Two air quality sites have been sampled extensively with the Delron cascade impactors beginning 1 September, 1976. Figure 3 details the location of the Kawishiwi Laboratories (Site #7003) and the Hoyt Lakes Golf Course (Site #7010). The Kawishiwi Laboratory is located ~18 km southeast of Ely, Minnesota. The laboratory lies ~200 m west of Highway 1 and ~50 m south of the Kawishiwi River in a heavily wooded area. Atmospheric particles were collected on the laboratory roof about 4 m above the ground where particle collection should not be appreciably affected by local ground activities or trees. Other sampling equipment present included an SO₂ and NO₂ bubbler and a high volume air sampler.

The Hoyt Lakes Golf Course is located ~2 km east of Hoyt Lakes, Minnesota in a moderately wooded area. The sampling station is situated ~15 m from an asphalt golf course drive and consists of a redwood platform ~2.5 m high. Other sampling equipment present included an SO₂ and NO₂ bubbler, a brushless high volume membrane sampler, an event rain sampler, and a bulk precipitation sampler. The sampling site lies ~10 km south of the Erie Mining Company tailing pond and taconite concentrator and ~3 km east of the Hoyt Lakes coal-fired power plant.

Metal Analysis of Cascade Impactor Stages

The cascade impactor slides and corresponding filters were removed from the impactors upon return to the laboratory and transferred to polycarbonate

Figure 3.
Cascade impactor sampling locations.



petri dishes which were appropriately labeled as to sampling site, date and impactor and stage number. The filters were removed from the glass slides with teflon-coated forceps and digested in 25-ml Teflon cups fit tightly in a stainless steel Paar Acid Digestion bomb. The digestion procedure is a modified version of a technique for decomposing marine particulates with HCl-HNO₃-HF acids. The original procedure (Eggemann and Betzer, 1976) calls for sequential addition of the three acids in a series of heating and cooling cycles. Studies in the laboratory have shown that simultaneous addition of the three acids reduced contamination introduced by repeated opening and closing of the bomb as required by the original procedure without reducing the quantitative nature of the digestion. Specifically 925 µl conc. HCl, 500 µl conc. HNO₃, and 75 µl conc. HF (Ultrex, Baker) were added to the filters in the teflon cups, and the bombs assembled. The digestion unit was heated at 95° ± 5° C in an oven for 3.5 hours and subsequently cooled in a freezer at ~-10° C for 45 minutes. After cooling, the bomb was carefully opened and the volume brought to 10 ml with the addition of 8.50 ml of mega-pure water. The contents of the cups were mixed by shaking and decanted into acid-washed polyethelene vials for analysis.

During the summer of 1977, it was discovered that contamination resulted in the above digestion procedure due to acid vapors seeping out of the teflon cup and attacking the stainless steel bomb. Subsequent migration of this material back into the cup caused occasional sample contamination. For this reason, lucite outer shells were machined and used in place of the stainless steel bombs for all samples collected subsequent to 1 July, 1977. Contamination problems were reduced significantly. Acid volumes were also increased during this period to 1000 µl, 1000 µl, and 100 µl for HCl, HNO₃, and HF, respectively.

To assess the quantitative nature of the digestion procedure, National Bureau of Standard Orchard Leaves were digested by the procedures described

above and analyzed for selected metals. The results obtained were compared to those listed on the certificate of analysis supplied by NBS. Percent recovery for each metal was calculated and the values are listed in Table 4. Recoveries were: Fe, 110%; Pb, 108%; Cu, 90%; Ca, 89%; Mg, 110%; Mn, 102%. Orchard Leaves' masses were chosen to yield metal values in the range to be expected for trace metals in air particulates. Although recoveries were good for all metals, the physical and chemical nature of Orchard Leaves will not be identical to that of air particulates. Thus, conclusions as to recoveries of the corresponding metals in air can only be speculative.

Metal blanks were prepared for evaluation by coating 0.6 μm pore-size 37 mm Nuclepore filters with Apiezon L as noted previously and digested according to the procedure described above. Blanks were determined by digestion in both stainless steel and lucite bombs. A new batch of Nuclepore filters was begun at the same time of conversion to lucite bombs; therefore filter blank values for the two cases are not directly comparable. The digested filters have contributions to metal blank values from grease, conc. HCl, HNO₃, and HF acids, the stainless steel bombs, and the filter. The first two sources contribute relatively constant metal quantities, while the bombs contribute variable quantities which were eliminated by conversion to lucite bombs. The metal contribution by the filters themselves is variable and accounts for most of the variations observed in this study. A study published by Wallace et al. (1977) after the bulk of this project was completed indicated that metal blank values in Nuclepore filters can be reduced significantly by an acid washing procedure.

All metals were analyzed with a Perkin-Elmer Model 360 Atomic Adsorption Spectrophotometer (AAS) equipped with a deuterium background corrector and an HGA-2100 Heated Graphite Atomizer. Metal standards were prepared by diluting 1000 ppm acidified stock solutions to the desired concentrations

TABLE 4

Recovery Studies of Metals in Standard Orchard Leaves

Metals	No. of Determinations	% Recovery	Std. Dev.
Pb	6	108	7.2
Fe	4	110	2.0
Cu	6	90	7.7
Ca	6	89	7.7
Mg	6	110	8.1
Mn	6	102	3.6

with mega-pure water. All standards were acidified with conc. HCl, HNO₃, and HF to match precisely the acid concentration of the digested impactor stages. In this manner, matrix errors in flameless AAS were minimized. In the case of Mn, it was discovered that the above standard solutions did not satisfactorily mimic the actual digested samples. Therefore, Mn was determined by running standard additions on one sample of each analytical set and the slope of this standard curve was used to calculate the Mn concentration in each sample.

Instrumental setting for the analysis of Cu, Ni, Pb, Fe, Mn, Al, Co, Cd, Ba, and Zn by flameless AAS are given in Table 5. Drying, charring, and atomizing times were typically 30, 20, and 8 seconds, respectively. For certain metals such as Fe, Al, Ca, and Mn, samples were diluted with mega-pure water to obtain signals in the linear response range of the instrument.

Detection limits for most metals analyzed were determined by the filter blank value and quantity of air samples rather than instrumental response. Detection limits listed in data tables were calculated as one standard deviation from the mean for six filter blanks and converted to ng/m³ air sampled for each individual collection episode.

Table 6 lists the concentrations given in µg/l and µg/filter for impactation filters digested in stainless steel and lucite bombs, and for back-up filters. Results between lucite and stainless steel bombs are not directly comparable as Nuclepore filters used are from different packages. Back-up filters typically had high blanks and poor reproducibility as seen in the table. Anomalously high values, not representative of the group, were not used in calculation of the mean values.

TABLE 5
 INSTRUMENTAL CONDITIONS FOR CASCADE IMPACTOR METAL ANALYSES

Metal	Drying Temp. (°C)	Charring Temp. (°C)	Atomization Temp. (°C)	Wavelength (nm.)
Cu	125	800	2700	324.7
Ni	125	800	2700	232.0
Pb	125	500	2200	217.0
Fe	125	1000	2700	248.3
Mn	125	1000	2700	279.5
Al	125	1400	2700	309.3
Co	125	900	2700	240.7
Cd	125	200	2300	228.8
Ca	125	1000	2700	422.7
Zn	125	400	2500	213.9

TABLE 6

METAL COMPOSITION OF NUCLEOPORE FILTER BLANKS ($\mu\text{g}/\text{l}^{\text{a}}$ or $\mu\text{g}/\text{filter} \times 10^{+2}$)

Impaction Filters-Digested in Stainless Steel Bombs							
	Fe	Al	Zn	Mn	Pb	Cu	Ni
	135	16.2	3.9	0.82	2.3	6.7	13.9
	140	11.2	3.1	0.62	2.3	8.8	27.1 ^b
	105	3.7	4.9	0.70	3.4	6.2	13.6
	77	7.3	3.8	0.62	1.4	7.3	8.4
	106	5.5	5.1	0.41	1.4	6.9	6.6
	107	10.5	22 ^b	0.41	2.0	32.6 ^b	6.0
Mean	112	9.1	4.2	0.60	2.1	7.2	9.7
Std. Dev.	23.8	4.5	0.8	0.16	0.8	1.0	3.8
Impaction Filters-Digested in Lucite Bombs							
	Fe	Al	Ca	Mn	Pb	Cu	Ni
	79	22	18	1.4	3.4	4.8	6.9
	46	16	23	1.2	6.1	3.3	5.4
	24	10	30	<1	2.2	3.7	2.6
	49	8.8	60	<1	2.8	6.0	19 ^b
	43	11	40	<1	2.5	7.3	12
	36	20	30	<1	6.8	4.9	4.5
Mean	47	15	34	0.4	4.0	5.0	6.3
Std. Dev.	18	6	15	0.7	2.0	1.5	3.6
Back-up Filters-Digested in Lucite Bombs							
	Fe	Al	Ca	Mn	Pb	Cu	Ni
	210	75	202	8.2	14	157	360 ^b
	150	42	148	7.2	39	340	50 ^b
	1760 ^b	92	143	94 ^b	530 ^b	2056	340 ^b
	180	58	100	7.0	21	230	21
	360	58	81	18	50	820	80
	100	75	57	37	25	44	18
Mean	200	67	122	16	30	607	42
Std. Dev.	98	18	53	13	15	758	29

^aConcentration based on 1 filter/10 mls solution^bNot included in calculation of mean

For all metals, duplicate injections were made for each sample, and the mean of the two injections was used to calculate the concentration of metal in the sample. If duplicate peaks were not within $\sim 10\%$ of each other, further injections were made until this condition was met. By this procedure, the mean value used does not vary by more than 5% from either of the two injections. Thus the analytical precision can be taken as $\sim 5\%$.

Tables A-1 through A-6, which correspond to the first two sampling dates, illustrate the effects of some of the problems encountered on earlier sampling episodes. Reproducibility of corresponding stages for impactors running side by side is poor in some cases.

Tables A-27 and A-28 contain metal concentrations for two impactors running side by side on the roof of the Space Science Center at the University of Minnesota, in Minneapolis. The values in Table A-27 were obtained from an uncovered impactor, while those from Table A-28 were from a covered impactor. The good agreement between the two tables for all metals, with the exception of copper, verifies the assumption that the protective cover does not significantly alter the collection properties of the impactor.

RESULTS AND DISCUSSION

INTRODUCTION

The objective of the completed research was to determine the size distribution of atmospheric particulate matter as to trace metal and sulfate content in northeast Minnesota. The sampling device chosen for collection of air particulates according to size was the Delron Cascade Impactor (Model DCI-6) which consisted of six impaction stages with cutoffs of 0.5, 1, 2, 4, 8, and 16 μm equivalent aerodynamic diameter plus a backup filter. The Delron sampler is a low-volume sampler with good stage resolution. Initially, the decision was made to determine the size distribution of air particulates for the metals Fe, Al, Mn, Cu, Ni and Pb. Throughout the course of the study, occasional analyses of Cd, Zn and Ca were performed to assist in interpretation of size distribution data. Unfortunately, atmospheric SO_4 concentrations are very low in NE Minnesota (0-2 $\mu\text{g}/\text{m}^3$) and no analyses are reported for its size distribution.

Observations on Particle Appearance

The general appearance of particles, especially color, were notably different as a function of stage collection. The first stage which collects large particles contained light-colored particulate matter distributed evenly across the surface of the impaction slide. In stages 1 through 6, particles appeared progressively darker and concentrated in the center of the glass slide and filter. The particulate matter on stage 6 which collects micron-sized particles was intensely black and concentrated in the stage center. The center accumulation was surrounded by a second concentric ring of dark particles while little or no material was observed on the stage perimeter. This pattern was easily noted on stages 4 through 6. The particles on the backup filter were uniformly distributed and varied from light in coloration to a grey-black.

The appearance of dark particles was most prominent in the fall and early winter of 1976 corresponding to a period of drought and forest/peat fire activity. Ward and Elliot (1976) report that the organic content (benzene soluble) of air particulates was correlated with periods of forest fire activity in Georgia, but was not correlated with suspended particulate concentration. As might be expected, particulates from forest fire would be small in size typical of a combustion source, black in color and enriched in organic carbon. Size distribution data shown in Table A-1 through A-7 (1976) (Appendix) for Al, Pb, Cu and Ni show no significant differences from data obtained in 1977 during a period of ample rainfall and little fire activity. Based on limited information, forest fire activity does not contribute significantly to Al, Pb, Cu and Ni concentrations in air particulates or their size distribution. Iron and Mn appear to be the exception in that most of the Fe and Mn in size-differential air particulates during 1976 appeared in the backup filter and therefore in sub-micron particles, in contrast to 1977 results which showed major large particle contribution.

Reproducibility of Sampling and Analysis

A comparison of selected metal concentrations in size-differentiated particulates for samples collected by Delron cascade impactors operated simultaneously side-by-side is given in Table 7. The metal concentrations were obtained by sampling for ~ 24-28 hours at the University of Minnesota atop the Space Science Center, at the Hoyt Lakes site and at the Kawishiwi Laboratory, followed by digestion and analysis of impaction stages.

Errors between individual stages or sampling unit were calculated based on the assumption that the mean of the two measured values was the actual concentration:

$$\begin{array}{l} \text{\% Error} \\ \text{(in 1 or 2)} \end{array} = \frac{|x_1 - (x_1 + x_2)/2|}{(x_1 + x_2)/2} \times 100$$

TABLE 7

VARIATION IN METAL SIZE DISTRIBUTION FROM
 CASCADE IMPACTORS OPERATED SIMULTANEOUSLY (ng/m³)

Set I - University of Minnesota (2/15/77)						
Size Range (μm)	Pb		Fe		Al	
	1	2	1	2	1	2
>16	73	68	920	940	1010	980
8-16	84	100	830	1610	830	970
4- 8	150	100	990	840	790	830
2- 4	110	130	640	600	1010	580
1- 2	120	120	460	740	470	650
.5- 1	200	140	380	410	640	330
<.5	1040	790	340	330	150	200
SUM	1777	1448	4560	5470	4900	4540
Set II - Hoyt Lakes (11/18/76)						
>16	3.1	2.3	1438	980	1135	766
8-16	4.2	3.0	1071	815	788	576
4- 8	6.7	3.0	892	645	614	388
2- 4	3.0	2.7	417	408	309	337
1- 2	3.9	3.9	238	261	191	201
.5- 1	3.2	2.7	102	162	91	96
<.5	<1	6	770	760	360	210
SUM	25	24	4928	4031	3488	2586
Set III - Kawishiwi Lab (3/22/77)						
>16	1.5	2.8	799	760	167	173
8-16	4.4	4.0	448	443	110	92
4- 8	3.4	4.1	351	266	94	157
2- 4	2.4	3.3	144	205	59	78
1- 2	3.4	3.1	114	120	69	56
.5- 1	3.1	2.8	40	60	44	90
<.5	2.8	<1	200	120	58	58
SUM	21.0	21.1	2096	1974	601	704

where X_1 and X_2 correspond to the concentrations of the metals in compared stages.

The error in total metal concentrations (sum of concentrations in six stages, plus backup filter) varied from 0.24% for Pb in Set III, collected at the Kawishiwi Laboratory, to 15% for Al in Set II, collected at Hoyt Lakes. Errors between individual stages varied from 0% for Al in the $<0.5 \mu\text{m}$ fraction in Set III to 71% for Pb in the $<0.5 \mu\text{m}$ size range in Set II. In general, errors between individual stages averaged 5-10%.

Differences in metal concentrations between stages of impactors operating simultaneously or in total metal collected may be the result of contamination in sample handling, collection characteristics of the impactor or analytical errors. The data in Table 7 reveal that neither impactor yielded consistently greater or lesser concentrations for a specific stage or metal. This observation suggests that contamination or analytical variability rather than sampling errors account for differences observed. Good agreement in total mass does not always correspond to agreement between individual stages. For example, 6 ng/m^3 Pb was found on the backup filter in Set II (Impactor #2) while the backup filter had 1 ng/m^3 Pb in Impactor #1 run simultaneously. However, the total sum of Pb concentrations for the two impactors were approximately equal. Particle bounce-off errors discussed previously have been invoked to explain similar occurrences in the literature, but are unlikely here, since analogous results were not observed for Fe and Al. In addition, the thin Apiezon L coating on the impaction surface is known to reduce particle bounce-off errors.

Metal Size Distributions

Size-differentiated air particulates from Hoyt Lakes and Kawishiwi Laboratory were analyzed routinely for Fe, Al, Ca, Mn, Pb, Cu and Ni. Complete data for all sampling events are presented in Tables A-1 through A-26 (Appendix). For comparison to urban patterns, metal concentrations for one sampling event at the University of Minnesota in Minneapolis are given in Tables A-27 and A-28.

Total metal concentrations obtained by summing the analytical values for the six impactor stages plus backup filter show considerable variation over the period of study and are summarized in Table 8. In general; metal concentrations at the Kawishiwi Laboratory averaged ~ 50-75% of the concentrations found at the Hoyt Lakes site. Of the metals determined, Fe concentrations were highest with means of 567 and 1507 ng/m³ at Kawishiwi Laboratory (KL) and Hoyt Lakes (HL), respectively. The large standard deviations observed at both sites illustrate the variability of particulate metal present for different sampling events. The factors controlling metal concentrations in air particulates are wind direction and velocity, frequency, duration and intensity of rainfall, and proximity to sources. Copper and Ni concentrations were lowest and generally undetectable in individual collection stages. As a result, Cu and Ni values listed in Table 8 are upper limits of actual concentrations.

The total metal concentrations shown in Figure 9 obtained by averaging the summations of stage metal concentrations for each site are compared to air particulate measurements obtained by membrane filtration (Eisenreich, et al., 1978). Although the values are not directly comparable because of differences in sampling location and frequency of sample collection, Mn, Pb, Cu and Ni concentrations are in reasonable agreement, whereas Fe and Al concentrations are significantly greater for those collected by cascade impaction. Calcium values are lower for the cascade impacter than means obtained by membrane filtration. Schmidt (1977) compared metal concentrations found in hi-vol samples and sums of impactor stages (Delron DCI-6) run concurrently on board ship on Lake Michigan. Agreement between values for filtered and impacted aerosols was fairly good for Ca, Cr, Fe, Mn and Pb, but poor for Al and Cu. Since hi-vol housings were made of Al and air pumps may have Cu parts, contamination for these two elements was possible. In general, total metal concentration in aerosols calculated by summing metal concentrations of individual

TABLE 8

TOTAL METAL IN CASCADE IMPACTOR SAMPLES*

Metal		Kawishiwi Lab**	Hoyt Lakes	University of Minnesota
Fe	Mean	567	1507	5015
	Max.	2096	4313	
	Min.	21.5	63	
	Std. Dev.	696	1749	
Al	Mean	418	752	4720
	Max.	932	2586	
	Min.	114	153	
	Std. Dev.	274	835	
Ca	Mean	192	327	3322
	Max.	411	759	
	Min.	24	47	
	Std. Dev.	136	281	
Mn	Mean	10	26	133
	Max.	34	98	
	Min.	3.7	2.8	
	Std. Dev.	6	33	
Pb	Mean	20	29	1613
	Max.	53	73	
	Min.	3.3	8.6	
	Std. Dev.	18	24	
Cu	Mean	<9.6	<9.8	21
	Max.	35	37	
	Min.	<0.6	<0.6	
	Std. Dev.	12	12	
Ni	Mean	<15	<24	90
	Max.	24	65	
	Min.	<6.8	<7.2	
	Std. Dev.	6.8	19	

* Sum of metal in seven impactor stages

** Not including sample date 11/18/76

TABLE 9

Comparison of Mean Total Metal Concentrations From
Cascade Impactor and Membrane Filter Analysis
Of Atmospheric Particulates

Metal	IMPACTOR ^a		MEMBRANE ^b		
	Kawishiwi	Hoyt Lakes	Hoyt Lakes	Fernberg	NE Minn.
	ng/m ³				
Fe	567	1507	991	376	1047
Al	418	752	157	100	240
Ca	192	327	215	201	-
Mn	10	26	11	6	15
Pb	20	29	31	19	58
Cu	< 9.6	< 9.8	2.8	4.8	6
Ni	< 15	< 24	0.5	1.2	2

^a Mean of total metal concentrations obtained by summing stage concentrations over study period - September, 1976 to December, 1977.

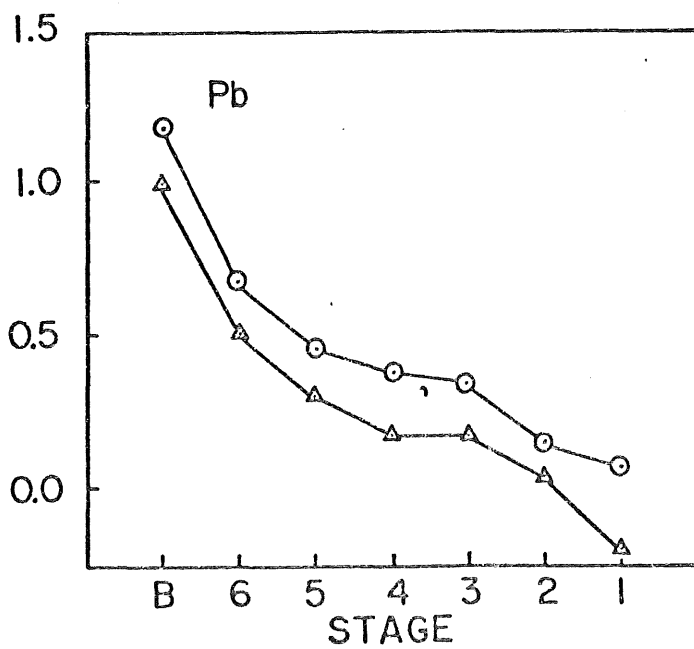
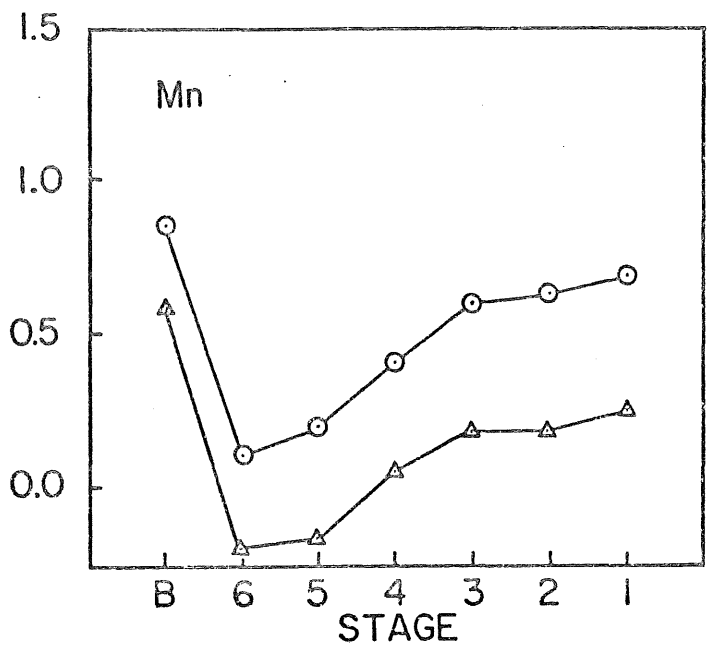
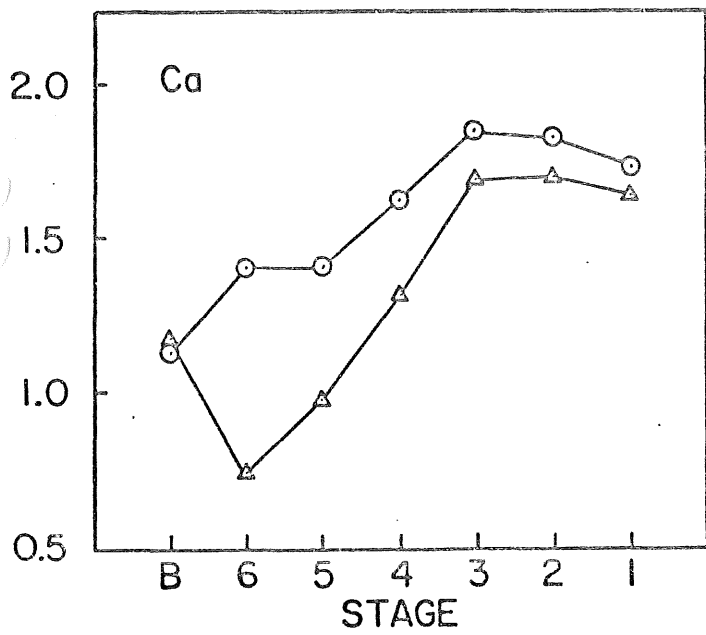
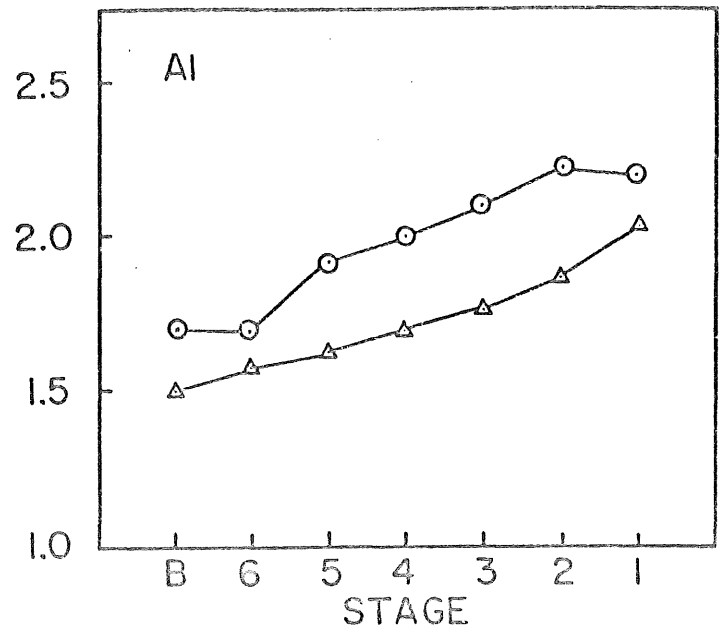
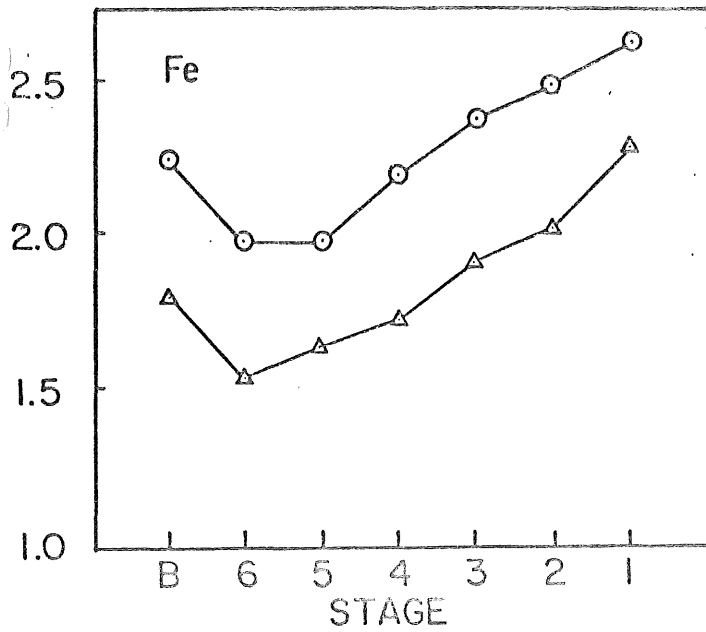
^b Data taken from Eisenreich et al., 1978; Mean of metal particulate concentrations obtained at Hoyt Lakes, a remote site at Fernberg and a lower estimate for NE Minnesota

stages may be assumed to correspond reasonably to total aerosol metal collected by membrane filtration. The higher Fe and Al total metal concentrations obtained from impactor measurements may be due to increased collection efficiency for large particles.

A comparison of size fractionated aerosol samples analyzed for metals at KL and HL and averaged over the study period is shown in Figure 4. The data is plotted as log of metal concentration versus impaction stage, with stage B representing the smallest particle size (backup filter), and stage 1, the largest particle size. Copper and Ni size distributions were not plotted since their concentrations in nearly all impactor stages analyzed were below detection.

The results of means for all size fractionated aerosols given in Figure 4 and Tables 10 and 11 indicate two clear trends. Iron, Al, Mn and Ca were nearly always dominated by large particle sizes while Pb occurred primarily in small particle sizes. Iron, Al, Ca and Mn concentrations exhibited a definite increase with increasing particle size, and Pb showed a distinct concentration increase with decreasing particle size. Iron and Mn concentrations tended, on the average, to increase in the $<0.5 \mu\text{m}$ size fraction. This pattern was identical at both sample collection sites, differing only in that metal concentrations were 2 to 3 times greater at HL than at KL. The increase in Fe and Mn concentration in the backup filter is indicative of a bimodal distribution for these elements, and suggests the presence of two specific sources. The higher concentrations exhibited at HL suggest that the primary source of metal-bearing aerosols originates in the vicinity of HL and is transported to the two sites by dispersion and wind. Since the aerosol would have to be transported a greater distance to KL, sedimentation and turbulent impaction would necessarily remove a significant percentage of the large particle size fraction, but would exert lesser influence

Figure 4.
Size distributions of Fe, Al, Ca, Mn and Pb in northeastern Minnesota aerosol. Points represent means calculated over sampling period.



○ Hoyt Lakes
 △ Kawishiwi
 log conc. (ng/m³)
 on ordinate

TABLE 10

MEAN ATMOSPHERIC METAL CONCENTRATIONS IN DIFFERENT SIZE FRACTIONS
AT KAWISHIWI LABORATORY (ng/m³)

Size Range (μm)	Fe	Al	Ca	Mn	Pb	Cu	Ni
>16	198 (258)	116 (90)	46 (35)	1.8 (0.97)	0.60 (0.61)	<1.3 (2.5)	<1.1 (0.49)
8-16	107 (153)	74 (56)	50 (36)	1.5 (0.93)	1.1 (1.5)	<4.5 (6.4)	<0.93 (0.30)
4- 8	83 (121)	59 (61)	49 (40)	1.5 (0.92)	1.5 (1.3)	<0.79 (0.95)	<0.93 (0.30)
2- 4	54 (57)	50 (37)	21 (20)	1.1 (0.44)	1.5 (1.0)	<0.53 (0.49)	<1.0 (0.24)
1- 2	44 (46)	47 (28)	9.5 (8.9)	0.67 (0.38)	2.1 (1.6)	<1.1 (2.1)	<1.2 (0.90)
.5- 1	34 (51)	39 (26)	5.5 (6.2)	0.66 (0.36)	3.2 (2.6)	<1.3 (2.9)	<1.1 (0.58)
<.5	61 (80)	60 (59)	15 (11)	3.8 (9.0)	10 (14)	ND	<8.4 (6.2)

TABLE 11

MEAN ATMOSPHERIC METAL CONCENTRATIONS IN DIFFERENT SIZE FRACTIONS
AT HOYT LAKES (ng/m³)

Size Range (μm)	Fe	Al	Ca	Mn	Pb	Cu	Ni
>16	443 (591)	162 (249)	53 (39)	4.8 (6.8)	1.2 (0.93)	<1.4 (1.5)	<2.2 (2.3)
8-16	304 (345)	168 (207)	69 (80)	4.2 (7.1)	1.4 (1.0)	<2.0 (3.0)	<2.0 (2.3)
4- 8	236 (267)	128 (142)	71 (74)	3.9 (4.9)	2.3 (1.6)	<1.0 (1.1)	<1.5 (0.96)
2- 4	158 (192)	104 (115)	43 (39)	2.6 (3.4)	2.4 (1.8)	<1.0 (1.6)	<1.4 (0.78)
1- 2	90 (115)	82 (85)	26 (39)	1.6 (1.5)	2.9 (1.9)	<2.7 (4.9)	<1.4 (0.78)
.5- 1	98 (157)	52 (43)	26 (24)	1.3 (1.0)	4.8 (3.6)	<1.9 (2.2)	<1.4 (0.78)
<.5	184 (258)	54 (65)	14 (6.5)	7.2 (9.2)	15 (15)	<0.60 ND	<14 (18)

on the fine particles. Ideally, such an explanation would require the metal concentrations to converge for the two sites as the particle size decreased (larger stage number). Manganese was the only metal that exhibited such a trend routinely. Aluminum showed a tendency to converge in the last three stages while Ca exhibited an opposing trend. Simple dilution of air particulates by atmospheric dispersion could account for the lower concentrations at KL and would not require distributions to converge if sedimentation and impaction losses were assumed negligible for all particle size ranges over the distance traversed. Since the majority of iron mining activities are located near HL, the size distributions point to mining-related activities as a possible source of Fe, Ca, Al and Mn in the study area. Lead is likely derived from the combustion of Pb-containing gasoline in automobiles. The size distribution pattern observed for Pb was constant with time, and similar to numerous studies performed in urban and remote areas (Duce et al., 1976; Schmidt, 1978; Lee and von Lehmden, 1973; Gladney et al., 1974; Nifong et al., 1972; Flocchini et al., 1976; Hardy et al., 1976; Cawse, 1974; Johansson et al., 1976; Martens et al., 1973; Pacinga and Jervis, 1976).

The prominent pattern exhibited by Fe and Mn indicate the presence of two sources - a large particle mode derived from natural sources (soil) and possibly mining activities, and a small particle mode of anthropogenic origin generated either locally or transported into the region from distant sources. Enhancement of the small particle size range at the expense of the large particles is known to occur in aged aerosols transported from a distant source (Pacinga and Jervis, 1976; Sverdrup et al., 1975).

Several meteorological factors can alter the physical size distributions of suspended particulates (Kapustin and Lyubovtseva, 1975). Increase in relative humidity can cause an increase in particle size due to adsorption of water. Sehmel and Sutter (1974) performed wind tunnel experiments which showed clearly

that wind speed greatly affected relative deposition velocities of different size fractions.

Additional information can be gained on metal aerosol behavior and source by considering interelement changes in different size fractions. Iron concentrations decreased more sharply than did Al and Mn as particle size decreased. Gladney et al., (1974) report that Al dropped off more sharply than Fe in U.S. east coast urban aerosol. In the present study, Mn concentrations decreased slightly through stage 3 then decreased sharply for particles $< 4 \mu\text{m}$. Although this characteristic was noted for both KL and HL, definitive explanations are not available. While Al and Ca concentrations were not enhanced in the $< 0.5 \mu\text{m}$ fraction in general, Mn and to a lesser extent, Fe increased in concentration. This behavior suggests strongly the presence of a small particle Mn and Fe source. Coal-fired power plants and high temperature taconite processes (e.g., pelletizing) are possible sources.

Calcium exhibited a significantly different distribution from Fe, Al and Mn although all four elements generally decreased in concentration with decreasing particle size. For Ca, the maximum in the large particle mode occurred between the cutoffs for stages 2 and 3 corresponding to $\sim 8 \mu\text{m}$ equivalent aerodynamic diameter. The maximum for the other metals was difficult to discern since the greatest concentration occurred in the first stage. Below stage 3, Ca concentrations decreased sharply, especially at Kawishiwi. Mean concentration for Ca at KL and HL are approximately equivalent in the $< 0.5 \mu\text{m}$ fraction. Calcium is thought to be derived from soil sources (wind-blown dust) and as such is expected to be dominated by particles having mass median diameters greater than $2 \mu\text{m}$. The relatively greater decrease in Ca concentration with decreasing particle size (increasing stage number) at KL suggests that losses in the small particle size range are greater than at HL. The heavy forest canopy

around KL may serve as an efficient scavenger of small particle Ca. Since this trend is not noted for Fe, Al and Mn, another explanation might be an additional source of Ca in the 0.5-2 μm size range (stages 2-6) at HL.

Lead concentrations increased with decrease in particle size through stage 6 (Figure 4). The backup filter which collects particles $< 0.5 \mu\text{m}$ generally accounted for greater than 50% of the total mass collected at both HL and KL. The lead distributions found for NE Minnesota were similar to those obtained in urban environments (Pacinga et al., 1975; Martens et al., 1973), remote continental environments (Sverdrup et al., 1975) and over Lakes Michigan (Schmidt, 1977) and Superior (Langevin et al., 1978). The distributions observed by Pacinga et al., (1975) and Martens et al., (1973) differed from those in this study in that stages prior to the backup filter showed constant or slightly decreasing concentrations with decreasing particle size. However, of the nine sites sampled by Martens et al., (1973), the Pb distribution at the rural site most closely resembled the data found in this study. Lead concentrations in urban areas reported in the literature were 10^1 to 10^3 times greater than the remote values of 20-30 ng/m^3 found in this study (Lee et al., 1972; Martens et al., 1973; Hardy et al., 1976). The lead concentrations reported were in good agreement with those obtained for similar sites in NE Minnesota - 10-20 ng/m^3 (Eisenreich et al., 1978) and the 25-40 ng/m^3 reported by Johansson et al., (1976) for aerosols collected in remote northern Florida.

The first two sampling events at KL in September, 1976 were not included in the calculation of mean distributions or concentrations. During autumn 1976, sampling at HL had not been initiated, thus comparison of data from the two sites was not possible. In addition, atmospheric conditions were not typical of "normal" trends in NE Minnesota. The region was experiencing a period of severe

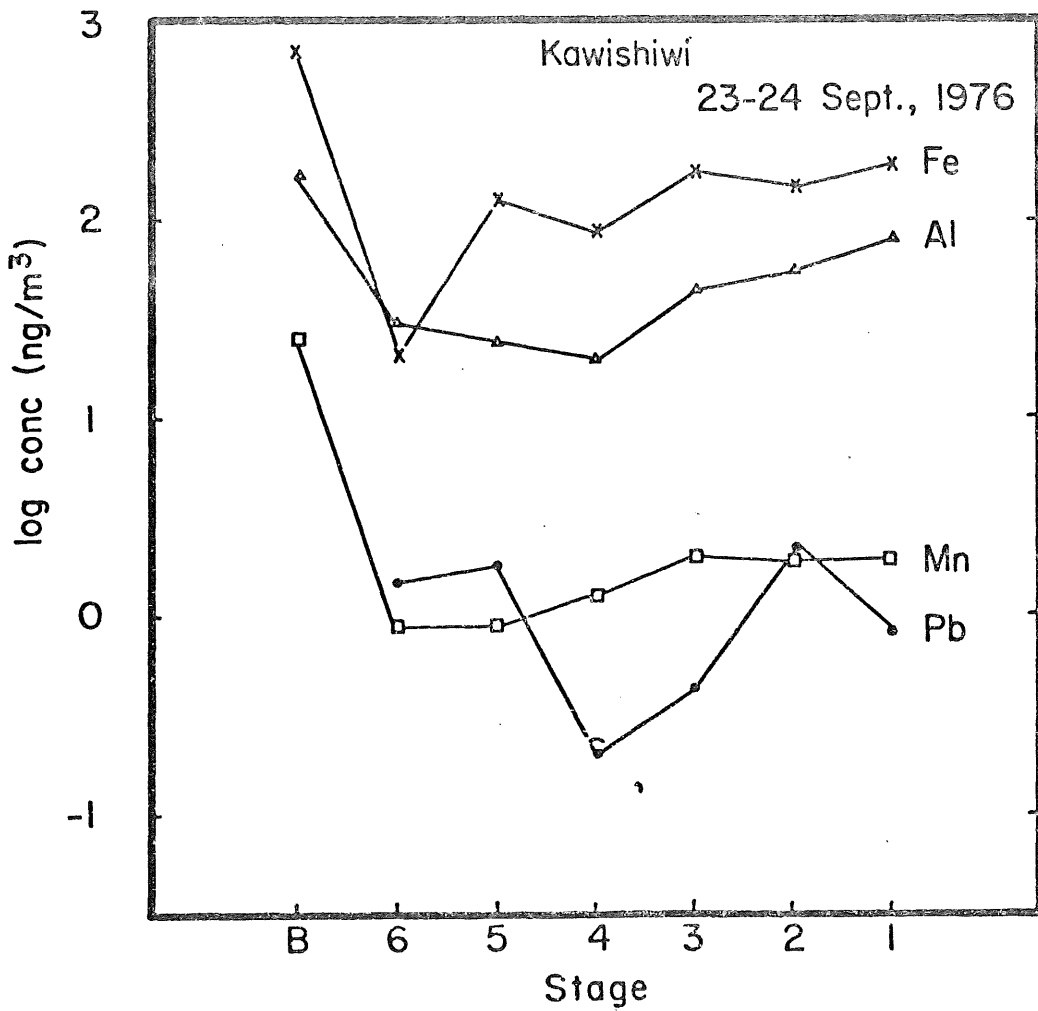
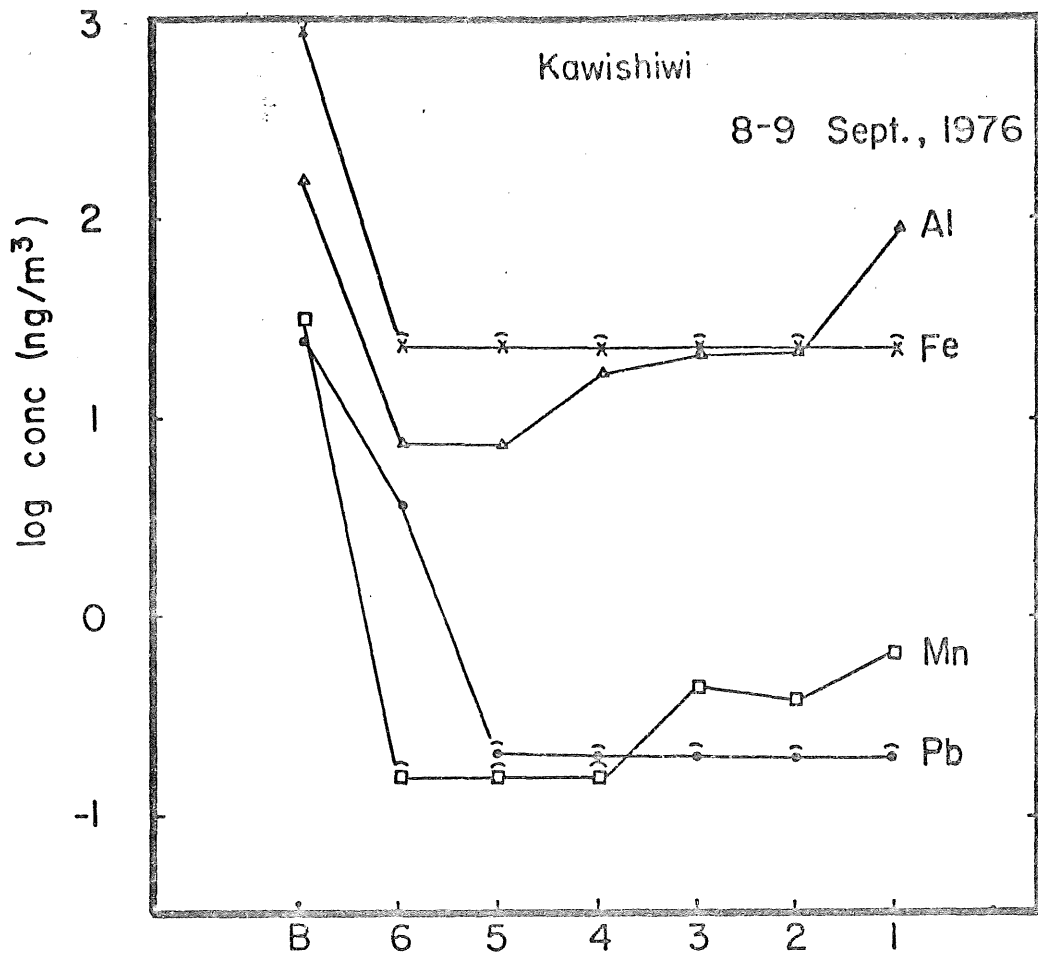
drought which resulted in numerous forest and peat/bog fires in the area. This condition continued through early November, 1976. Little information is available on the metal composition or size distribution of smoke particles derived from forest fires. The dry conditions were also conducive to extensive entrainment of small particle soil dust. Since washout and turbulent impaction are the primary mechanisms for the removal of small-particles from the atmosphere (Friedlander, 1977), the lack of rain precluded their efficient removal. Air particulate metal concentrations in the small particle range could be expected to remain high until rain occurred or a cleaner air mass moved into the region.

Metal size distributions for the first two sampling events is shown in Figure 5. On 8 September, 1976, Fe was below detectable concentrations for stages 1 through 6, but increased dramatically in the backup filter. Aluminum and Mn distributions were consistent with distributions found for later sampling dates. As with Fe, Al, Mn and Pb concentrations increased in the $< 0.5 \mu\text{m}$ fraction. A similar distribution was observed for 23 September, 1976, although concentrations were greater in the $72 \mu\text{m}$ fraction than the earlier date.

The data from 18 November, 1976 taken at KL were also not included in the calculation of distribution parameters. The samples were apparently contaminated by a fuel oil furnace malfunction at KL. The concentrations of Fe, Al, Mn, Pb and Ni were higher on this occasion than on any other during the sampling period (Table A-7), Appendix A). On this data, total Ni was 1212 ng/m^3 , which was typically less than 15 ng/m^3 . Size distributions deviated from the observed pattern as Fe, Mn, Pb and Ni had maxima in stages 3 and 6. This data is included here as an example of possible contamination patterns from local sources

In an effort to obtain detectable concentrations of metals normally evading detection (Cu, Ni, etc.), an extended sampling time of 21-27 May, 1977 was employed. Air particulate samples were collected at KL, HL and near the Dunka Road site (Erie Mining Co.). Impactors at HL and Dunka Road yielded no useful

Figure 5.
Metal particle size distribution in late summer, 1976. Samples collected on 8-9, Sept. and 23-24, Sept. at Kawishiwi Lab. Particle size increases from left to right.



information as insects drawn into the air stream obstructed air flow. Concentrations for the elements determined are given in Table 12. Cobalt and Cu were undetectable ($< 0.1-0.2 \text{ ng/m}^3$) in all stages; Ni was undetectable in 3 of 7 stages. Size distributions for Ca, Fe, Al, Mn, Pb, Cd and Zn are illustrated in Figure 6. Both Cd and Zn in air particulates exhibited bimodal distributions with maxima in stages 1 and 6 with a valley in stage 3. Distributions for Ca, Fe, Al, Mn and Pb were similar to the means discussed previously.

Elemental Enrichment Factors

Atmospheric aerosols collected near the earth's surface in remote continental areas may be expected to have the earth's crust as their major natural source. By comparing the composition of the collected aerosol to the composition of the earth's crust, information as to the contribution of the crust to the total composition of the aerosol can be obtained. In the same manner, the relative contribution of anthropogenic sources to the metal composition of the aerosol may be estimated. The comparison is conveniently obtained by calculation of elemental enrichment factors for various elements in aerosols as compared to crust material. The general formula for the calculation of enrichment factor is (Rahn, 1976):

$$EF(X)_{\text{aerosol-source}} = \frac{(X/_{\text{Ref}})_{\text{aerosol}}}{(X/_{\text{Ref}})_{\text{source}}}$$

where $EF(X)_{\text{aerosol-source}}$ is the enrichment factor of element X in the aerosol relative to a source reference element, and $X/_{\text{Ref}}$ is the ratio of the concentration of element X to a reference element in the aerosol or source material. Elements commonly used as reference elements in crustal matter are Al, Ti, Si, Fe, Ce and Sc. Elements having enrichment factors close to unity are in crustal proportions

Figure 6.
Metal particle size distribution in spring, 1977. Sample collected
on 21-27 May at Kawishiwi Lab. Particle size increases from left
to right.

KAWISHIWI

21-27 May, 1977

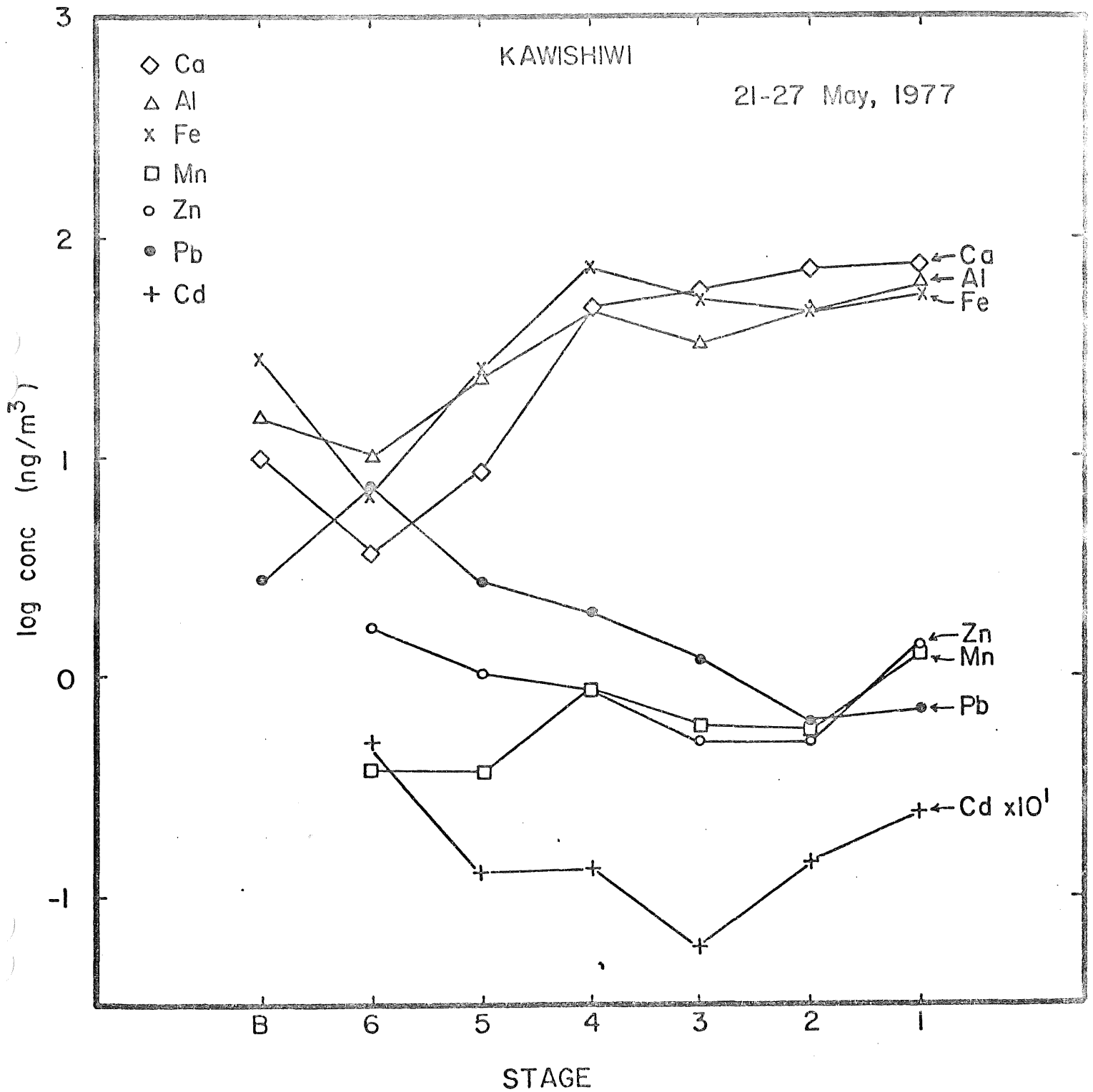


Table 12: Atmospheric Metal Size Distribution at Kawishiwi Lab. (ng/m³)

Size Range (μm)	Fe	Al	Ca	Mn	Pb	Cu	Ni	Cd	Co	Zn
>16	52	64	75	1.22	0.72	<0.1	1.2	0.024	<.2	1.4
8-16	48	47	69	0.56	0.64	<0.1	<0.3	0.016	<.2	.5
4-8	54	33	58	0.60	1.2	<0.1	<0.3	0.006	<.2	.5
2-4	76	47	48	0.90	2.0	<0.1	1.4	0.013	<.2	.9
1-2	26	23	8.7	0.30	2.7	<0.1	<0.3	0.012	<.2	1.1
.5-1	6.7	10	3.8	0.40	7.6	<0.1	<0.3	0.050	<.2	1.7
<.5	28	15	10	<.5	2.8	ND*	<3	ND	<.2	ND
M _T	291	239	273	4.05	17.7	<0.6	<6.8	.12	<1.4	6.1
MMD (μm)	4.6	6.5	8.4	6.6	1.2			1.89		2.87
r ²	.97	.99	.95	.99	.91			.98		.97

Impactor 3 Sampling Period: 5/21-27/77 Sample Volume: 107.81 m³ Wind: SE 5-15+

* ND - Not Determined

to crustal reference elements, and may be assumed to have the crust as a major source. Such elements are referred to as nonenriched, while those elements having EF's significantly greater than unity may be assumed to have a major source other than the earth's crust. In effect, elements with large EF's are thought to be derived from anthropogenic activities.

Aluminum was chosen as the crust reference element in this study for several reasons (Rahn, 1976): 1) Al is a major component of crustal material 2) Al is a minor component of pollution aerosols; 3) Al can be detected easily by routine analytical instrumentation; 4) Al is generally free of contamination in sampling. Iron is also a popular crustal reference element, but is a major component of pollution aerosols. Ideally, a crustal reference element should have negligible pollution sources and be unreactive in the atmosphere. In addition Fe would be of little value as a crustal reference in NE Minnesota where taconite iron mining is prevalent. Thus aerosol-crust enrichment factors used here were calculated by the formula:

$$EF_X = \frac{(X/Al)_{\text{aerosol}}}{(X/Al)_{\text{crust}}}$$

Crustal abundances were chosen over soil composition because rocks have been more extensively analyzed than soils, and soil composition may vary significantly even over a small geographical area. Crustal abundances for most elements have been compiled by many researchers including Mason (1966), Taylor (1964) and Goldschmidt (1958). Table 13 shows the crustal abundances reported by Taylor (1966) and the (element/Al) ratio for all elements.

The use of elemental enrichment factors have several limitations which must be appreciated before interpretation is made. For example, EF's near unity for an element means only that the element occurs in crustal proportions to Al; this does not necessarily mean that it is derived from a crustal or

TABLE 13
ELEMENTAL COMPOSITION OF EARTH'S CRUST^a

Component	Crustal Abundance	Normalized to Al
F	625 ppm	0.0076
Na	2.83%	0.348
Mg	2.09%	0.257
Al	8.13%	1.000
Si	27.72%	3.41
P	1050 ppm	0.0129
S	260 ppm	0.0032
Cl	130 ppm	0.0016
K	2.59%	0.319
Ca	3.63%	0.447
Ti	4.40%	0.541
V	135 ppm	0.0017
Cr	100 ppm	0.0012
Mn	950 ppm	0.0117
Fe	5.00%	0.615
Co	25 ppm	3.08×10^{-4}
Ni	75 ppm	9.23×10^{-4}
Cu	55 ppm	6.77×10^{-4}
Zn	70 ppm	8.61×10^{-4}
As	1.8 ppm	2.21×10^{-5}
Se	0.05 ppm	6.15×10^{-7}
Br	2.5 ppm	3.08×10^{-5}
Ag	0.07 ppm	8.61×10^{-7}
Cd	0.2 ppm	2.46×10^{-6}
Sn	2.0 ppm	2.46×10^{-5}
Sb	0.2 ppm	2.46×10^{-6}
I	0.5 ppm	6.15×10^{-6}
Cs	3.0 ppm	3.69×10^{-5}
Ba	425 ppm	5.23×10^{-3}
La	30 ppm	3.69×10^{-4}
Ce	60 ppm	7.38×10^{-4}
Au	0.004 ppm	4.92×10^{-8}
Hg	0.08 ppm	9.84×10^{-7}
Pb	13.0 ppm	1.60×10^{-4}
Bi	0.2 ppm	2.46×10^{-6}

^aMason (1966)

natural source. In polluted areas, anthropogenic sources may emit crustal material (fly ash, road dust), but may have EF's near unity. Atmospheric concentrations may be a better indication in this case.

High EF's in polluted areas are attributed almost exclusively to anthropogenic sources. However, high EF's in remote areas may be due to natural soils enriched in a particular element, action of unrecognized natural sources (forest fires, vegetation) and transport of pollutants from urban areas. Probably the most significant limitation is the fact that the precursor of the crustal material is not yet known. For this reason, EF's of 1 to 10 may simply be artifacts of using the wrong reference element.

Elemental EF's using Al as a reference element were calculated for metals in impactor stages (Tables 10-11) at KL and HL are given in Table 14. Zinc and Cd EF's were calculated from data obtained during the sampling period 21-27 May, 1977 at KL.

EF's close to unity indicate negligible enrichment compared to Al, and may be of crustal (natural sources) origin. Geographic variations in soil composition can account for EF's deviating slightly from unity. For example, in Table 14 Fe, Ca and Mn have EF's between 0.5 and 3.0 in stages 1 through 6 suggesting that large particle Fe, Ca and Mn may be attributed to entrainment of natural material by natural or man's activities (mining, road traffic, etc.). This conclusion is consistent with the particle size distributions presented earlier.

Iron and Mn were enriched in the $< 0.5 \mu\text{m}$ fraction at both KL and HL. The increase in EF in the $< 0.5 \mu\text{m}$ fraction is consistent with the hypothesis that small particle metal is derived from man's activities and thus should be enriched over crustal abundances. Iwasaki (personal communication, 1978) has indicated that blasting, crushing and consolidation stages of taconite mining and processing produce fine particles which may be enriched in Fe. The EF's

for Ca were near unity corroborating previous evidence that Ca is soil derived. In fact, regional soil may be depleted in Ca. Alternately, the existence of a small particle Al source is suggested. Aluminum, Fe and Mn in atmospheric aerosols are also derived from coal-fired power plants (Gladney et al., 1974).

The EF's observed for Pb increased with decreasing particle size ranging from a minimum of 37 (large particle) to a maximum of 1735 (small particles). The overall EF for Pb in NE Minnesota based on impactor analysis was ~ 250 , indicating significant enrichment compared to Al, but still below the global average of ~ 1500 (Rahn, 1976). The mean EF for Pb obtained from membrane filtration data in NE Minnesota was 1233-1510. Small particle Pb is derived from gasoline combustion. Both Cd and Zn were enriched in aerosols, primarily in small particles. Maximum EF's were noted in the $< 0.5 \mu\text{m}$ fraction-2032 for Cd, 197 for Zn. In general, enrichment factors were greatest for all elements studied in the $< 0.5 \mu\text{m}$ fraction. However, Fe, Al, Ca and Mn concentrations were dominated by large particles, and Pb, Cd and Zn by small particles.

The EF's discussed above represent a mean for the region during the study period. Relative concentrations of Al, Ca, Mn and Pb did not vary considerably during this period. However, Fe exhibited large fluctuations in EF relative to Al during the period of interest. Figure 7 shows the variation in Fe EF's relative to Al in each impactor stage at HL and KL over the study period. EF's ranged from 144 in stage 1 in the winter 1977 at HL to < 0.1 in late 1977 sampling dates. The EF of unity is drawn on each graph in Figure 7 depicting relative changes over time. Stage EF's falling on this line correspond to un-enriched Fe; points above the line, Fe is enriched, and points below the line, Fe is depleted, or Al is enriched.

Prior to late July, 1977, all aerosol samples collected exhibited Fe EF's greater than or equal to unity at both sites. Aerosols sampled subsequent to late July, 1977, EF's were less than or equal to unity. This trend is noted

Figure 7.
Crustal enrichment factor for Fe as a function of particle size and time.

ENRICHMENT FACTOR

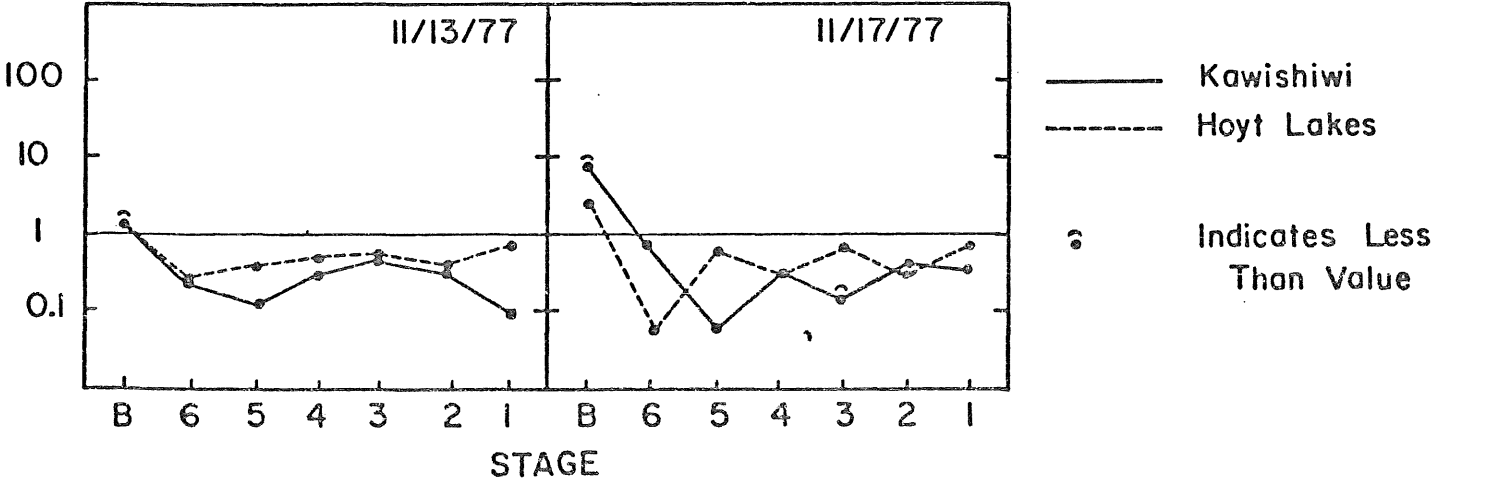
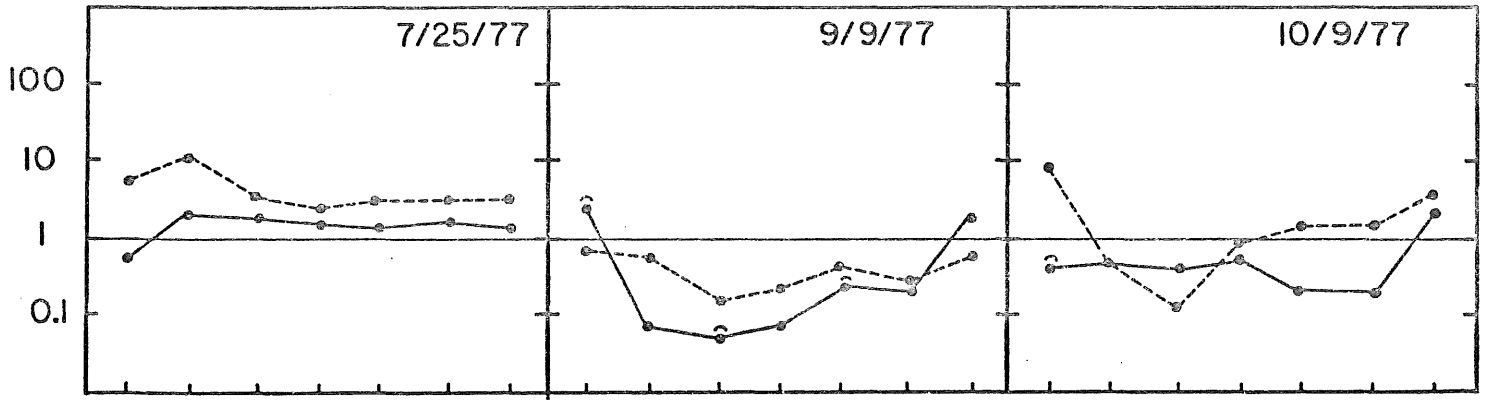
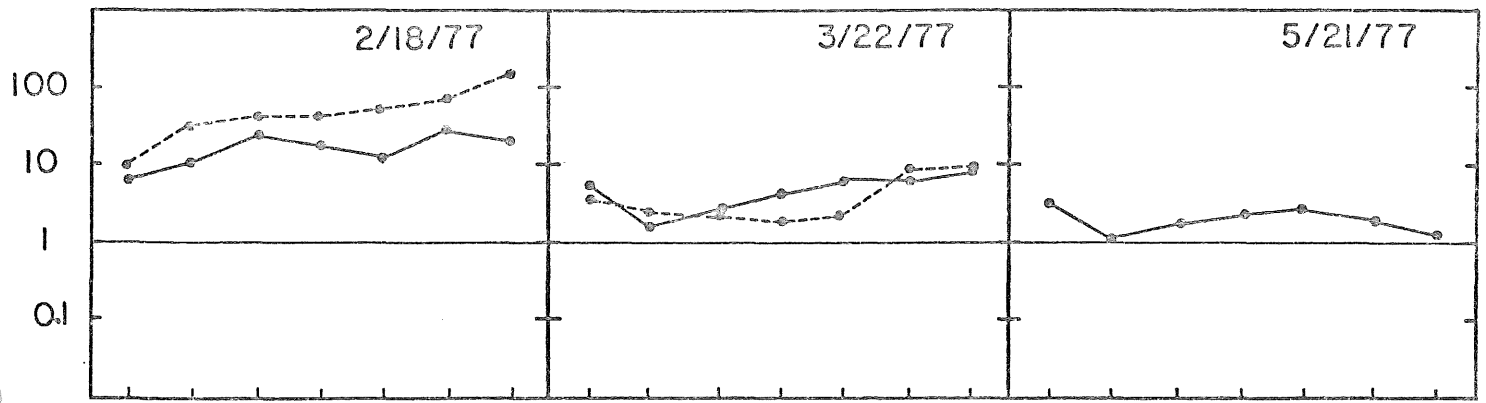
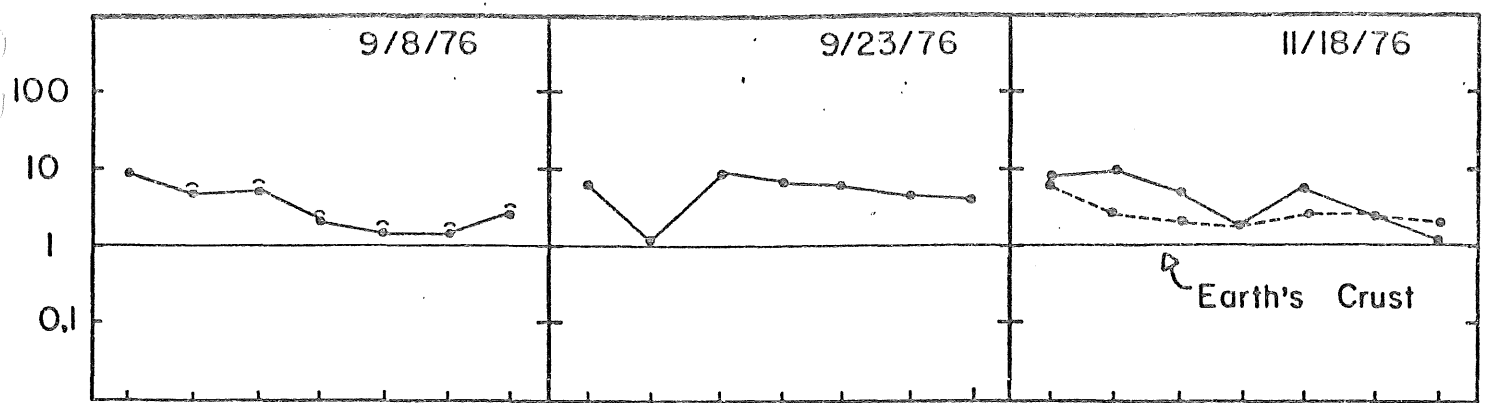


TABLE 14

METAL ENRICHMENT FACTORS AT KAWISHIWI LAB. AND HOYT LAKES

Size Range (μm)	Fe		Al		Ca		Mn		Pb		Cd	Zn
	HL	K	HL	K	HL	K	HL	K	HL	K	K	K
>16	4.4	2.7	1.0	1.0	.73	.94	2.5	1.3	46	37	152	25
8-16	2.9	2.5	1.0	1.0	.92	1.7	2.1	1.8	52	103	138	12
4- 8	3.0	2.4	1.0	1.0	1.2	2.0	2.6	2.2	112	150	74	18
2- 4	1.3	2.0	1.0	1.0	.93	1.1	2.1	2.1	144	185	112	22
1- 2	1.8	2.0	1.0	1.0	1.6	.56	1.7	1.7	221	313	212	56
.5- 1	3.0	1.5	1.0	1.0	1.1	.35	2.1	1.6	576	554	2032	197
<.5	5.5	5.6	1.0	1.0	.58	.60	11	11	1736	1042	-	-

easily in Figure 7 where EF's for Fe are nearly all below the crustal reference line. The dramatic reversal of the EF trend for Fe as a function of particle size coincided with a shutdown of taconite mining activities in NE Minnesota because of a strike. Whether the change in Fe EF was a result of actual mining activities or a decrease in vehicle traffic on dirt roads cannot be surmised from this data. However, resuspended particles resulting from vehicle movement on dirt roads or blowing wind may be the major source of air particulates in the region (K. Whitby, personal communication, 1978). Interestingly, Fe EF's in the $<0.5 \mu\text{m}$ size fraction were not significantly different from pre-shutdown periods.

Calculation of Mass Median Diameters

Mass median diameters (mmd) have been calculated for each sampling event utilizing a program applied to an HP-97 calculator. The program consists of two distinct operations; first, an inverse normal integral subprogram was written which converted percentage metal below each size cutoff to a probability scale assuming a log normal distribution; secondly, a linear regression routine was incorporated to calculate a best fit for a line derived from a probability versus log particle size. The program and application procedure is given in Appendix B. For cases in which all of the mass occurred in either the first stage or backup filter, mmd's were not calculated by the program, but approximated by assuming an upper or lower cutoff for the first and last stage, respectively. Tables A-1 through A-28 (Appendix A) list mmd's for each metal determined in each sample run. A correlation coefficient (r^2) is also listed for each mmd which is a measure of the degree of log normality for each metal size distribution. Correlation coefficient values near unity imply a log normal distribution. Inspection of the data reveal that r^2 values range between 0.9 and 1.0. In most instances, deviations of r^2 from unity are suggestive of a bimodal or trimodal

distribution. Willeke and Whitby (1975) report that aerosol particle volume, mass and number are not log normally distributed across all particle sizes, but only within each major size mode - Aitkin nuclei, Accumulation and Coarse Particle.

The mean mmd's are listed in Table 15 for Fe, Al, Ca, Mn and Pb based on mean metal size distributions for HL and KL during the study period. As expected from size distributions, Fe, Al, Ca and Mn yielded mmd's greater than 4 μm in all cases. The mmd's for Al, Ca and Pb were greater at KL than at HL. Mn mmd's at the two sites were approximately the same, while Fe mmd was less at KL than at HL. The large mean mmd observed for Ca at KL strongly suggests the presence of a nearby soil component near KL, perhaps a nearby dirt road. Iron mmd's varied considerably with sampling event at both sites with the mean mmd slightly greater at HL. The mmd observed for Fe of $\sim 7 \mu\text{m}$ is relatively large compared to previously published values (Table 1), even for urban sites. Cawse (1974) obtained a low value for Fe mmd ($\sim 2.5 \mu\text{m}$) at a remote site in England. Schmidt (1977) observed a mean mmd range of 3.8-5.6 over Lake Michigan while urban values were $\sim 2.8-3.6$. Schmidt (1977) suggested that mmd's obtained with Delron cascade impactors (DCI-6) may be high due to inherent flow properties, wall losses and inaccurate cutoff calibration under the conditions of impactor use. Schmidt (1977) has determined Pb mmd's for the Delron cascade impactor and a slot-type, jet impactor run simultaneously. Schmidt (1977), concluded that the Delron impactor may overestimate the Pb mmd by $\sim 0.5 \mu\text{m}$. However, Whatman 41 filters were used as an impaction surface. In this study, mmd's determined at the University of Minnesota for Fe, Al, Mn, Ca and Pb were typical of urban values supporting the data obtained in NE Minnesota. In addition, the mmd for total aerosol (mass) determined with the Minnesota electrical aerosol analyzer agreed fairly well with the Fe mmd in this study (C. Wilson, personal communication, 1978). At the present time the accuracy of the determined mmd's is open to question due to the existence of conflicting information.

TABLE 15

MASS MEDIAN DIAMETERS (μm) OF PARTICULATE METAL IN NE MINNESOTA

Metal		Kawishiwi Lab.	Hoyt Lakes	University of Minnesota
Fe	Mean	6.9	7.3	5.2
	Max.	>16	10.3	
	Min.	~.25	3.8	
	Std. Dev.	5.8	2.7	
Al	Mean	4.9	4.5	5.3
	Max.	9.8	7.8	
	Min.	0.69	3.5	
	Std. Dev.	3.0	1.5	
Ca	Mean	7.8	5.2	6.9
	Max.	14.9	7.7	
	Min.	5.5	2.7	
	Std. Dev.	3.7	1.9	
Mn	Mean	5.2	5.0	0.47
	Max.	17.2	8.1	
	Min.	0.08	0.08	
	Std. Dev.	5.1	3.3	
Pb	Mean	1.1	0.91	0.38
	Max.	3.0	2.6	
	Min.	0.04	0.18	
	Std. Dev.	1.1	0.88	

The smallest mmd's were found for Pb at 1.1 and 0.91 μm at KL and HL, respectively. Other studies (Table 1) have reported mmd's ranging from 0.42-3.4 μm for Pb, agreeing well with the ranges for NE Minnesota.

Copper and Ni, largely undetectable in air particulates from NE Minnesota did not yield sufficient stage mass to routinely determine mmd's. For those values calculated, copper mmd's ranged from 2.5-7.5 μm at KL and 0.73 to 3.5 μm at HL. Due to high blank levels, it was not possible to determine Cu in the back-up filter; therefore, actual mmd's may be lower than the values reported in Tables A-1 through A-28.

Zinc, Cd, and Co were determined on the sample collected 21 May, 1977 at KL (Table 12). Cobalt was not detectable in any stage; thus no MMD is reported. Mass median diameters were 2.87 and 1.89 μm for Zn and Cd, respectively. The Zn value was higher than the range reported by other researchers (Table 1).

Temporal Variations in Metal Particle Size

The variation in Fe and Pb aerosol mmd's over the period of study is presented for HL and KL in Figure 8. Iron was chosen for the analysis of temporal variations as it corresponds to particulates derived from natural sources and mining activities while Pb represents anthropogenically-derived aerosol. The relatively small number of sampling events precludes any definitive conclusions to be drawn as to seasonal trends. However, the mmd for Fe appears to increase over time at KL, but remains constant at HL. In both cases, there is a noticeable decrease in Pb mmd over the study period. This trend becomes very dramatic after July, 1977 following shutdown of taconite mining and processing.

Temporal trends in aerosol behavior can be better examined by considering concentration changes with time as a function of particle size. Figures 9 and 10 show plots of Fe, Al and Pb concentrations in particle sizes larger and smaller than 2.0 μm . The cutoff of 2.0 μm was chosen to represent the mass of Fe, Al and Pb occurring in the respirable fraction ($< 2.0 \mu\text{m}$) and to delineate the influence of large and small particle-size sources.

Figure 8.
Log mmd (Fe and Pb) at Kawishiwi Lab and Hoyt Lakes as a function of
time.

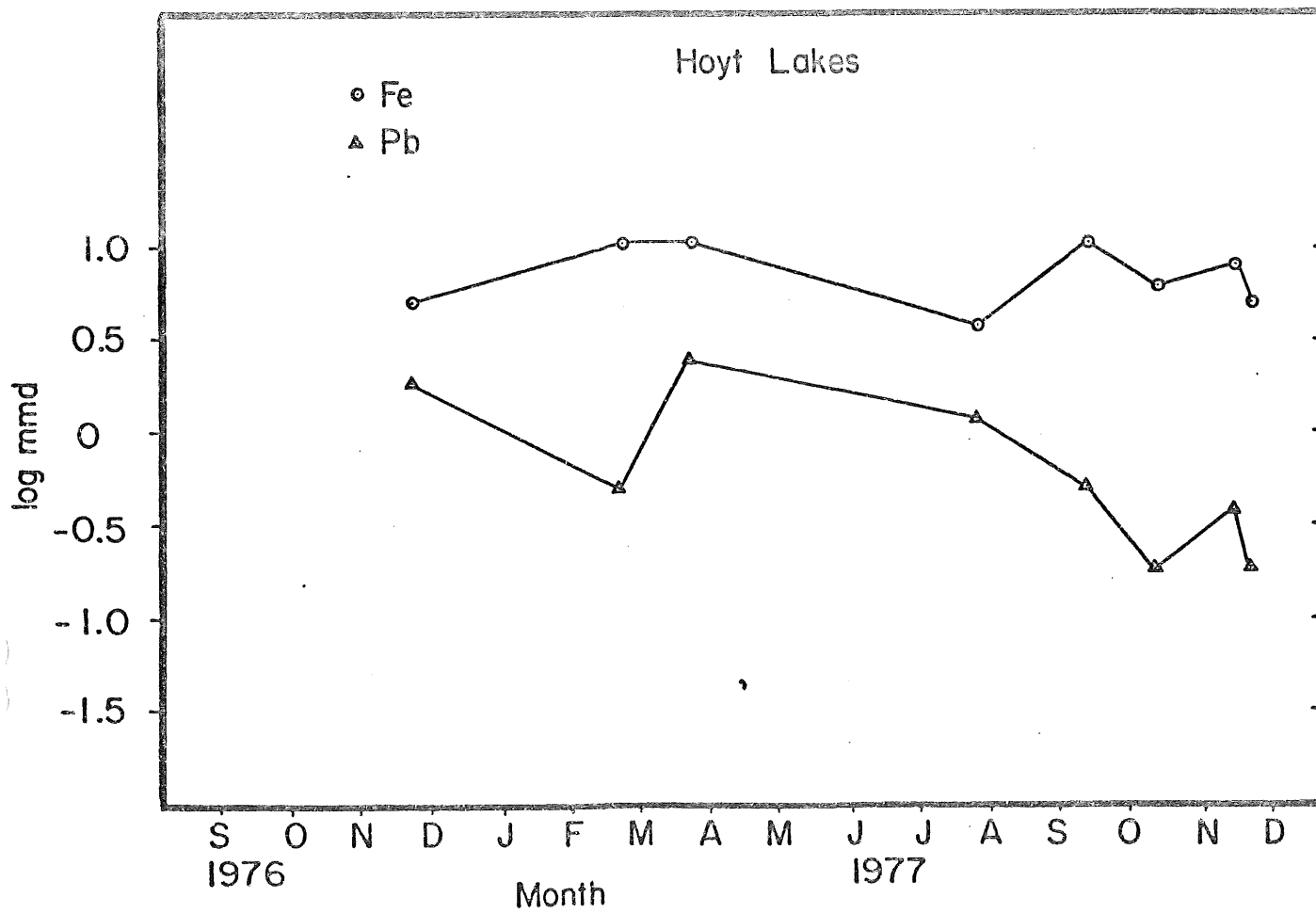
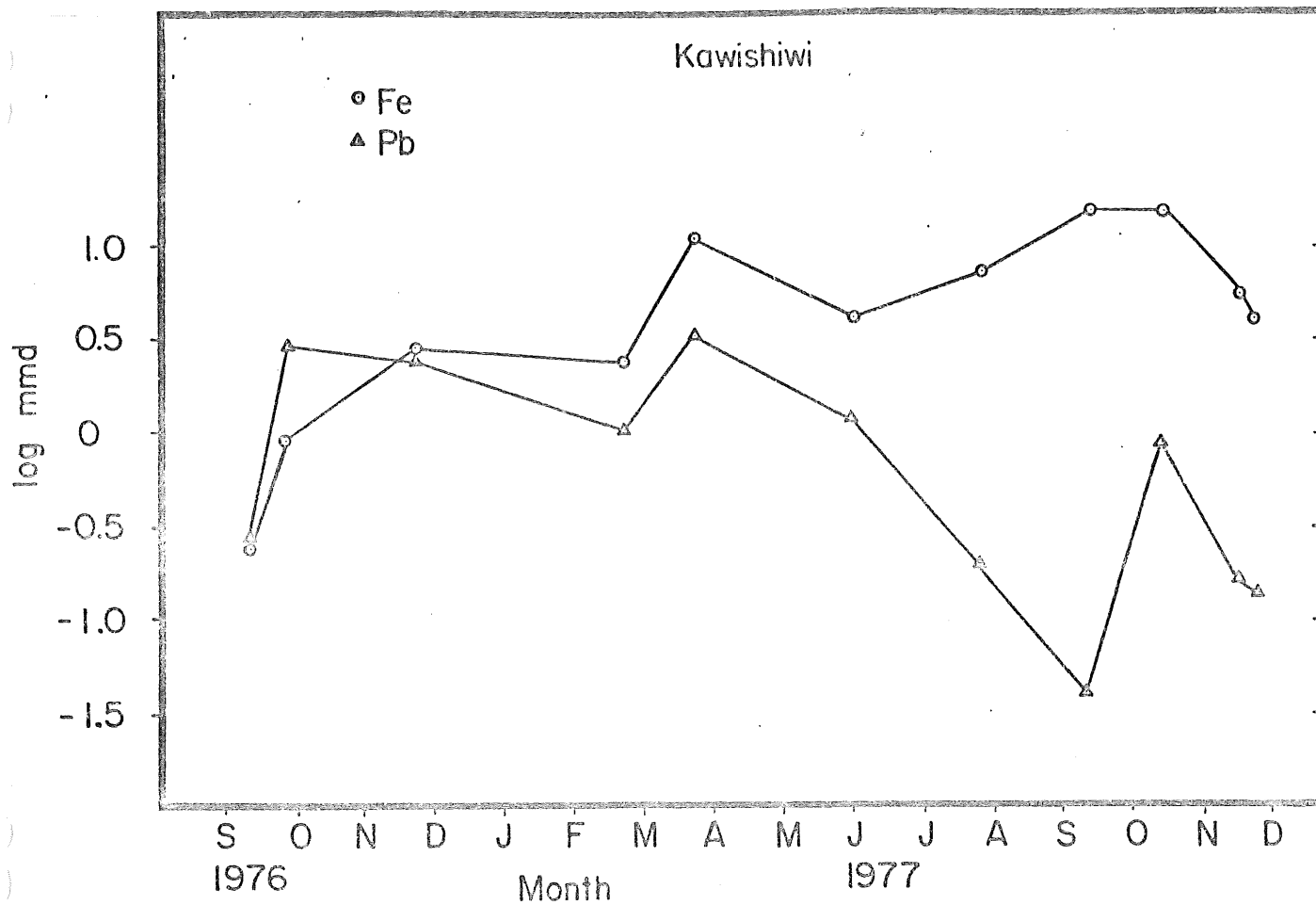


Figure 9.
Iron, Al, and Pb concentrations greater than and less than 2 μm diameter
as a function of time at Kawishiwi Lab.

KAWISHIWI

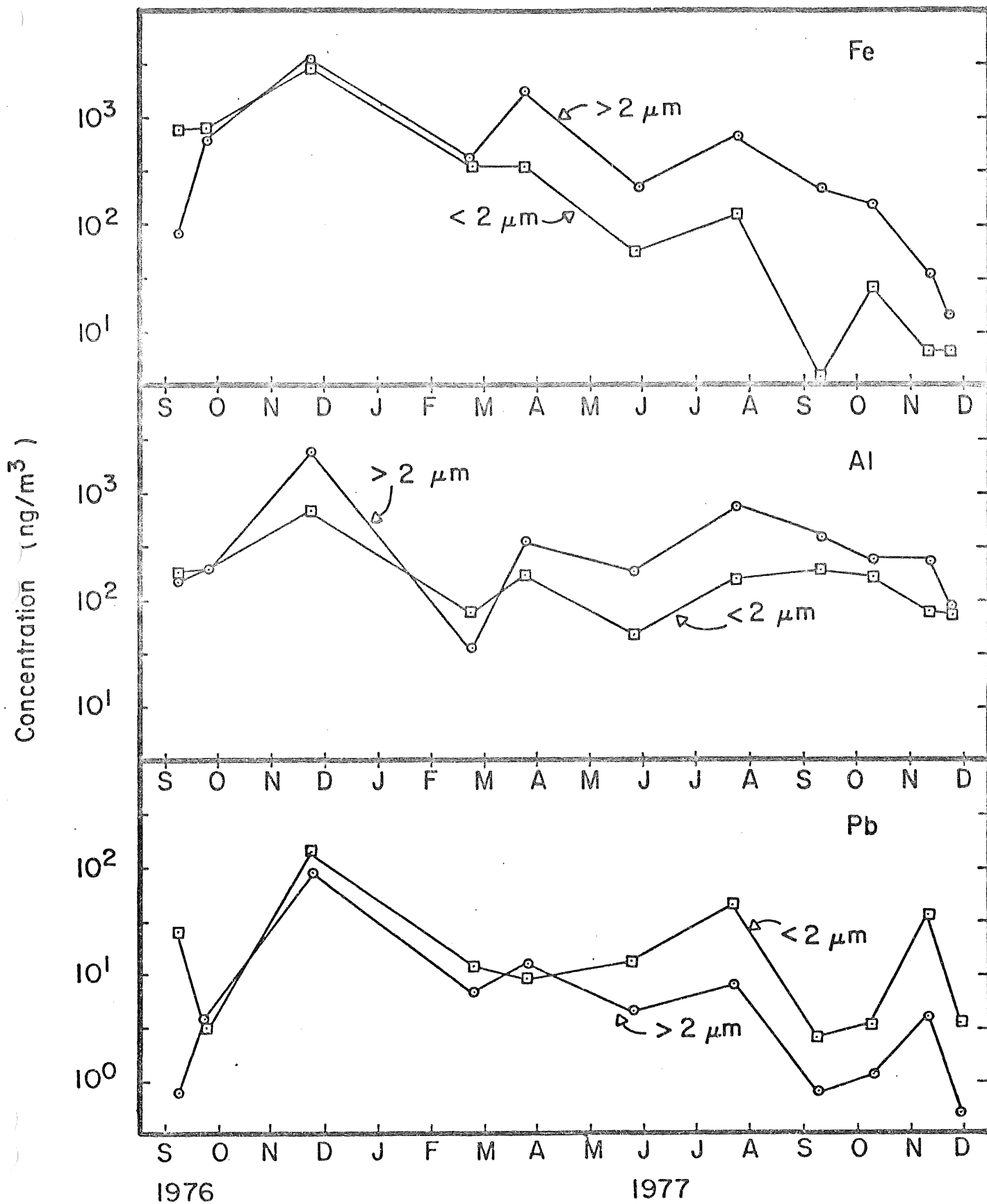
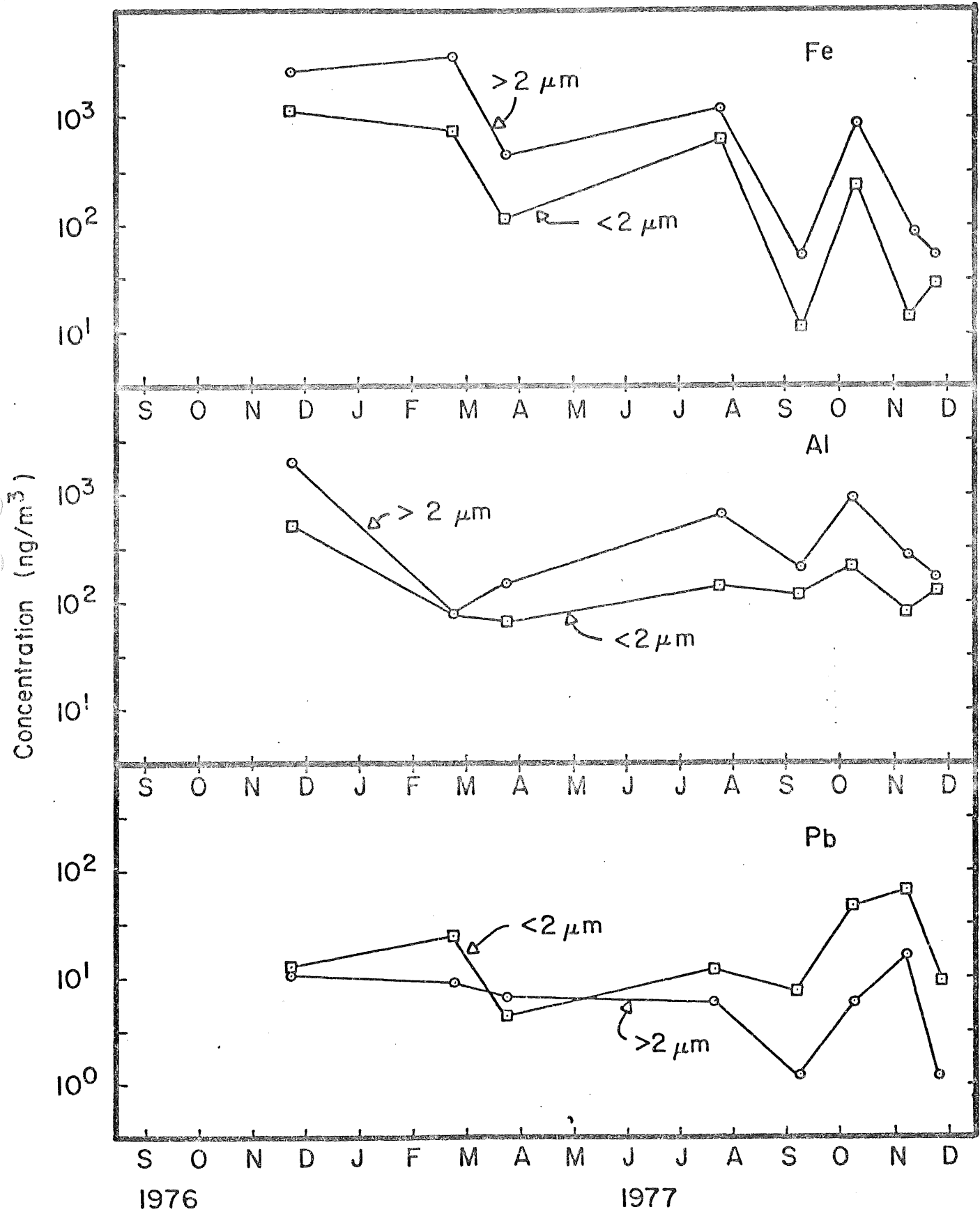


Figure 10.
Iron, Al, and Pb concentrations greater than and less than 2 μm diameter
as a function of time at Hoyt Lakes.

HOYT LAKES



AT KL and HL, the concentrations of Fe and Al were dominated by the size fraction greater than 2.0 μm diameter. At KL, the difference between the $>2 \mu\text{m}$ and $<2 \mu\text{m}$ fraction increases dramatically subsequent to March, 1977 for Fe, Al and Pb. In addition, Fe concentrations decreased after July, 1977, but total Al concentrations as well as the proportion in each size fraction remained constant. This data suggests that the sources of atmospheric particulate Al and Fe were not the same. The trend is noted also at HL, but not to such a significant extent, probably due to the proximity of the HL site to an urban source.

Lead concentrations in the <2 and $>2 \mu\text{m}$ fractions at HL and KL were about the same prior to May, 1977. Subsequently, the $<2 \mu\text{m}$ fraction became the primary concentration mode for Pb at both sites. The total concentrations at both sites reached a minimum in September, 1977 corresponding to a period of heavy rainfall and washout from the atmosphere. Rainfall after September, 1977 was meager permitting the buildup of higher aerosol Pb concentrations.

Dry Deposition Rates

The input of atmospheric materials to natural systems (land, vegetation, water) via fallout may have a significant impact on the receptor. The severity of impact will be in part, dependent on the magnitude of the fallout and of the composition of the material deposited. Thus far, this report has dealt with the metal composition of size-differentiated aerosols. An assessment of dry deposition rate of the metals analyzed for is performed. As already mentioned, Cawse (1974) has related deposition velocities to mmd . Other works include the direct measurement of deposition velocities of monodisperse uranine particles onto a water surface (Sehmel and Sutter, 1974), and a study of metal deposition onto grass fields and smooth teflon surfaces (Davidson, 1977).

Measurements by Sehmel and Sutter (1974) were performed in a laboratory wind tunnel and can be expected to differ somewhat from the actual processes

taking place in the environment. Experiments by Sehmel and Sutter (1974) are most applicable to this study since elemental deposition to a water surface is of primary interest in the wilderness area of the Boundary Waters Canoe Area (BWCA). The data obtained by Sehmel and Sutter (1974) is presented as a plot of particle deposition velocity vs particle diameter (Figure C-1). Since deposition velocity is not a linear function with particle size, deposition velocities based on mmd only provide a crude estimate of dry deposition rate. In this study, each cascade impactor stage, and therefore particle size range was treated separately as to deposition velocity. From Figure C-1, a deposition velocity for a particular particle diameter can be chosen for a variety of wind speeds. Knowing the particle deposition velocity and the metal concentration in a size range, the dry deposition rate can be calculated according to Chamberlain (1960):

$$\phi = X \cdot V_g$$

where ϕ = flux density or dry deposition rate

(mass deposited/unit area-unit time)

X = atmospheric particulate metal concentration directly above collection surface (mass per unit volume)

V_g = deposition velocity (length/unit time).

The detailed procedure for determining deposition rates based on analysis of particle size ranges is given in Appendix C.

Dry deposition rates were calculated from the mean metal concentrations in each stage at HL and KL over the study period (Table 16). Dry deposition rates were calculated for Fe, Al, Ca, Mn, Pb, Cu, Ni, Zn, Cd and Co for two wind speeds - 2.2 and 7.2 m/sec. The average wind speed in NE Minnesota is \sim 4 m/sec (W. Enderson, personal communication, 1978).

Metal loadings in Table 16 are compared with dry and bulk loadings from Eisenreich et al., (1978). The bulk values include both dry and wet deposition and the total should be somewhat greater than dry deposition alone. If the dry loading at 2.2 m/sec wind speed is assumed to be more representative of environmental conditions, all metals, with the exception of Al and Fe, agree well with the bulk deposition values as determined by Eisenreich et al., (1978). Since the Fe and Al dry deposition rates of Eisenreich et al., are also significantly greater than the corresponding bulk rates, there is reason to doubt the accuracy of Fe and Al bulk deposition values. Metals found primarily on large particles (Fe, Al, Mn, Ca) would be expected to have a significant dry deposition contribution to bulk loading, whereas metals found on small particles (Zn, Pb, Ni, Cu) would be deposited primarily by wet deposition).

Dry loading, as determined in this study was greatest for Fe, with values of 1.2-19.6 kg/ha-yr and 2.7-46.0 kg/ha-yr at Kawishiwi and Hoyt Lakes, respectively. (Range of loadings discussed corresponds to the range of wind velocities). Smallest loading was found for Cd, 0.15-2.5 kg/ha-yr at KL. It should be noted that Cd, Zn, and Co loadings in Table 16 are based on one sampling event (5/21-27/77) and therefore may not be representative of the entire sampling period.

A comparison of dry deposition estimates made by numerous investigators to different environments is given in Table 17. The dry deposition estimates calculated in this study and by Eisenreich et al. (1978) for the region based on x-ray fluorescence analysis of air particles are less than those observed for most regions of the U.S. and Europe with one important exception. Dry deposition of Fe in NE Minnesota appears to be of the same order of magnitude as that observed in industrialized areas. Based on this comparison and seasonal variations of Fe enrichment in air particulates (Figure), it appears that taconite

iron mining and related activities contributes significantly to the total Fe atmospheric burden and deposition in the region.

TABLE 16
 ATMOSPHERIC LOADING OF TRACE METALS
 IN NORTHEASTERN MINNESOTA (kg/ha-yr)

	Kawishiwi Lab ¹		Hoyt Lakes ¹		Northeastern Minnesota ²	
	2.2m/sec	7.2m/sec	2.2m/sec	7.2m/sec	Dry ^a	Bulk ^b
Fe	1.2	19.6	2.7	46.0	4.9	0.28
Al	0.70	11.9	1.1	18.6	0.89	0.26
Ca	0.31	5.4	0.38	6.6	-	<5.3
Mn	0.012	0.20	0.031	0.53	0.023	-
Pb	0.0055	0.088	0.0095	0.15	0.017	0.050
Cu	<0.012	<0.24	<0.010	<0.18	0.009	0.008
Ni	<0.0074	<0.12	<0.015	<0.25	0.008	<0.010
Zn	0.008	0.14	-	-	0.055	0.041
Cd	0.00015	0.0025	-	-	0.0025	0.003
Co	<0.0014	<0.024	-	-	0.0020	-

¹ This study

² Eisenreich et al. (1978)

a Calculated based on atmospheric concentration and Vg from Cawse (1970)

b Measured utilizing a bulk deposition collector

TABLE 17

Comparison of Dry Deposition Estimates For Atmospheric Particulates

Metal	This Study		Eisenreich et al., (1978)	Schmidt (1977)	Andren and Lindberg (1977)	Cawse (1974)	Winchester and Nifong (1971)	Gatz (1975)
	KL	HL						
Kg/ha-yr								
Fe	1.2	2.7	4.9	7 - 64	-	1.3	16.5	0.53
Al	0.7	1.1	0.89	3.2 - 24	-	1.4	8.6	0.24
Ca	0.31	0.38	-	19 - 140	-	4.4	7.1	-
Mn	0.012	0.031	0.023	.01 - .67	.01 - .22	0.05	0.88	0.01
Pb	0.0055	0.0095	0.017	.26 - 2.1	.05 - 1.4	0.12	0.42	0.04
Cu	<.012	<.010	0.009	.14 - 1.2	.002 - .13	<.02	0.61	0.017
Ni	<.007	<.015	0.008	-	-	<.02	0.19	0.002
Zn	0.008	-	0.055	-	-	0.25	0.75	0.02
Cd	0.00015	-	0.0025	-	-	<.04	0.002	0.0007
Co	<0.0014	-	0.002	-	-	0.001	0.01	-

REFERENCES

1. Andren, A. W. and Lindberg, S. E. (1977), Atmospheric Input and Origin of Selected Elements in Walker Branch Watershed, Oak Ridge, Tennessee. *Water, Air and Soil Poll.*, 8, 199-215.
2. Blifford, I.H., Jr., and Gillette, D. A., (1971), Applications of the Lognormal Distribution to the Chemical Composition and Size Distribution of Naturally Occurring Atmospheric Aerosols. *Water, Air and Soil Poll.* 1, 106-114.
3. Blifford, I. H., Jr., and Gillette, D. A., (1972), The Influence of Air Origin on the Chemical Composition and Size Distribution of Tropospheric Aerosols. *Atmos. Environ.* 6, 463-480.
4. Cawse, P. A.. (1974), A Survey of Atmospheric Trace Elements in the U.K. (1972-1973). AERE Harwell Report No. R7669.
5. Chamberlain, A. C., (1960), Aspects of the Deposition of Radioactive Gases and Particles. In *Aerodynamic Capture of Particles*. Pergamon Press, London.
6. Chester, R., Aston, S. R., Stoner, J. H., and Bruty, D., (1974), Trace Metals in Soil-Sized Particles From the Lower Troposphere Over the World Ocean. *J. Rech. Atmos.* 8, 777-789.
7. Davidson, C. I.. (1977), Deposition of Trace Metal-Containing Aerosols on Smooth, Flat Surfaces and on Wild Oat Grass (*Avena fatua*). Ph.D. Thesis, Cal. Institute of Technology, Pasadena, Calif.
8. Duce, R. A., Ray, B. J., Moffman, G. L., Walsch, P. R. (1976), Trace Metal Concentration as a Function of Particle Size in Marine Aerosols from Bermuda. *Geophys. Res. Lett.*, 3 (6), 339-342.
9. Dzubay, T. G., Hines, L. E., and Stevens, R. K. (1976), Particle Bounce Errors in Cascade Impactors. *Atmos. Environ.* 10, 229-234.
10. Dzubay, T. G. and Steven, K., (1975), Ambient Air Analysis With Dichotomous Sampler and x-ray Fluorescence Spectrophotometer. *Environ. Sci. Technol.* 9(3), 663-668.
11. Edgington, D. N. and Robbins, J. A. (1976), Records of Lead Deposition in Lake Michigan Sediments Since 1800. *Environ. Sci. Technol.* 10(3), 266-274.
12. Eggimann, D. W. and Betzer, P. R. (1976), Decomposition and Analysis of Refractory Oceanic Suspended Materials. *Anal. Chem.* 48(6), 886-890.
13. Eisenreich, S. J., Langevin, S. A., and Hollod, G. J. (1978), Elemental Composition and Deposition of Air Particulates and Precipitation in Remote Northern Minnesota, Report to Minnesota Environmental Quality Council, Cu-Ni Regional Study.

14. Faoro, R. B. and McMullen, T. B. (1977), National Trends in Trace Metals in Ambient Air 1965-1974. EPA-450/1-77-003.
15. Flocchini, R. G., Cahill, T. A., Shadoan, D. J., Lange, S. J., Eldred, R. A., Feeney, P. J., Wolfe, G. W., Simmeroth, D. C. and Suder, J. K. (1976), Monitoring California's Aerosols by Size and Elemental Composition. Environ. Sci. Technol. 10 (1), 76-82.
16. Friedlander, S. K. (1977), Smoke, Dust and Haze; Fundamentals of Aerosol Behavior, John Wiley and Sons, New York.
17. Gatz, D. F. (1975), Pollutant Aerosol Deposition into Southern Lake Michigan. Water, Air, Soil Pollution 5, 239-251.
18. Gladney, E. S., Zoller, W. H., Jones, A. G., and Gordon, G. E. (1974), Composition and Size Distributions of Atmospheric Particulate Matter in Boston Area. Environ. Sci. Technol. 8 (6), 551-557.
19. Goldschmidt, V. M. (1958), Geochemistry, Oxford University Press, pp. 74-75.
20. Graedel, T. E. and Franey, J. P. (1974), Atmospheric Aerosol Size Spectra: Rapid Concentration Fluctuations and Bimodality. J. Geophys. Res. 79 (36), 5643-5645.
21. Huntzicker, J. J., Friedlander, S. K., and Davidson, C. L. (1975), Material Balance for Automobile-Emitted Lead in Los Angeles Basin. Environ. Sci. Technol. 9 (5), 448-457.
23. Johansson, T. B., Van Grieken, R. E., and Winchester, J. W. (1976), Elemental Abundance Variation with Particle Size in North Florida Aerosols. J. Geophys. Res. 81 (6), 1039-1046.
24. Kadowaki, S. (1976), Size Distribution of Atmospheric Total Aerosols, Sulfate, Ammonium and Nitrate Particulates in the Nagoya Area. Atmos. Environ. 10, 39-43.
25. Kapustin, V. M. and Lyubovtseva, A. S. (1975), Relative Humidity and the Parameters of Natural Aerosols. Atmos. and Ocean Physics 9 (2), 570-574.
26. Langevin, S. A., Eisenreich, S. J., and Johnson, T. (1978), Trace Metals in Air Particulates, Rain, Surface Films, and Water on Lake Superior. In preparation.
27. Lee, R. E., Jr., and Goranson, S. (1972), National Air Surveillance Cascade Impactor Network. I. Size Distribution Measurements of Suspended Particulate Matter in Air. Environ. Sci. Technol. 6 (12), 1019-1024.
28. Lee, R. E., Jr., Goranson, S., Enrione, R. E., and Morgan, G. B. (1972), National Air Surveillance Cascade Impactor Network. II. Size Distribution Measurements of Trace Metal Components. Environ. Sci. Technol. 6 (12), 1025-1030.

29. Lee, R. E. and von Lehmden, D. J. (1973), Trace Metal Pollution in the Environment. *J. Air Pollution Control Assoc.* 23 (10), 853-863.
30. Liu, B. Y. H. and Lee, K. W. (1976), Efficiency of Membrane and Nuclepore Filters for Submicrometer Aerosols. *Environ. Sci. Technol.*, 10 (4), 345-350.
31. Ludwig, F. L. and Robinson, E. (1968), Variations in Size Distributions of Sulfur-Containing Compounds in Urban Aerosols. *Atmos. Environ.* 2, 13-23.
32. Lundgren, D. A. (1967), An Aerosol Sampler for Determination of Particle Concentration as a Function of Size and Time. *JAPCA* 17, 225-229.
33. Lundgren, D. A. (1971), Determination of Particulate Composition, Concentration and Size Distribution Changes with Time. *Atmos. Environ.* 5, 645-651.
34. Marple, V. A. and Liu, B. Y. H. (1974), Characteristics of Laminar Jet Impactors. *Environ. Sci. Technol.* 8 (7), 648-654.
35. Marple, V. A. and Willeke, K. (1976), Impactor Design, *Atmos. Environ.* 10, 891-896.
36. Martens, C. S. (1973), Ion Ratio Variations with Particle Size in Puerto Rican Aerosols. *J. Geophys. Res.* 78 (36), 8867-8871.
37. Martens, C. S., Weslowski, J. J., Kaifer, R., and John, W. (1973) Lead and Bromine Particle Size Distributions in the San Francisco Bay Area. *Atmos. Environ.* 7, 905-914.
38. Mason, B. (1966), *Principles of Geochemistry*, 3rd Ed., Wiley and Sons, Inc., New York.
39. Miller, D. F., Levy, A., Pvi, D. Y. H., Whitby, K. T., and Wilson, W. E., Jr. (1976), Combustion and Photo Chemical Aerosols Attributable to Automobiles. *JAPCA* 26 (6), 576-581.
40. Mitchell, R. I. and Pilcher, J. M. (1959), An Improved Cascade Impactor for Measuring Aerosol Particle Sizes. *Ind. Eng. Chem.* 51, 1039-1042.
41. Nifong, G. O., Boettner, E. A., and Winchester, J. W. (1972), Particle Size Distributions of Trace Elements in Pollution Aerosols. *Amer. Ind. Hyg. Assoc. J.*, 33, 569-575.
42. Pacinga, J. J. and Jervis, R. E. (1976), Multi-element Size Characterization of Urban Aerosols. *Environ. Sci. Technol.* 10 (12), 1124-1128.
43. Pacinga, J. J., Roberts, T. M., and Jervis, R. E. (1975), Particle Size Distributions of Lead, Bromine, and Chlorine in Urban-Industrial Aerosols. *Environ. Sci. Technol.* 9 (13), 1141-1144.
44. Rahn, K. A. (1976), *The Chemical Composition of the Atmospheric Aerosol*. Graduate School of Oceanography, Univ. of Rhode Island.

45. Schmidt, J. (1977), Selected Metals in Air Particulates Over Lake Michigan. Master's Thesis, Water Chemistry Dept., Madison, Wis.
46. Sehmel, G. A. and Sutter, S. L. (1974), Particle Deposition Rates on a Water Surface as a Function of Particle Diameter and Air Velocity. *J. Rech. Atmos.* 8, 911-920.
47. Sverdrup, G. M., Whitby, K. T., and Clark, W. E. (1975), Characterization of California Aerosols - II. Aerosol Size Distribution Measurements in the Mohave Desert. *Atmos. Environ.* 9, 483-494.
48. Taylor, W. R. (1964), Abundance of Chemical Elements in the Continental Crust; A New Table. *Geochem. Cosmochem. Acta.* 28, 1273-1285.
49. Wallace, G. T., Jr., Fletcher, I. S., and Duce, R. A. (1977), Filter Washing, A Simple Means of Reducing Blank Values and Variability in Trace Metal Environmental Samples. *J. Environ. Sci. Health* A12 (9), 493-506.
50. Ward, D. E. and Ellito, E. R. (1976), Georgia Rural Air Quality: Effect of Agricultural and Forestry Burning. *J. APCA*, 26 (3), 216-220.
51. Whitby, K. T., Clark, W. E., Marple, V. A., Sverdrup, G. M., Sem, G. J., Willeke, K., Liu, B. Y. H., and Pui, D. Y. H. (1975). Characterization of California Aerosols - I. Size Distributions of Freeway Aerosol. *Atmos. Environ.* 9, 463-482.
52. Whitby, K. T. (1977), The Physical Characteristics of Sulfur Aerosols, "Particle Technology Laboratory Publication No. 335," Univ. of Minn., Whitby, K. T., Liu, B. Y. H., and Kittelson, D. B., pp. 1-51.
53. Willeke, K. and Whitby, K. T., Atmospheric Aerosols: Size Distribution Interpretation. *J. APCA.* 25 (5), 529-534 (1975).
54. Winchester, J. W. and Nifong, G. D. (1971), Water Pollution in Lake Michigan by Trace Elements from Pollution Aerosol Fallout. *Water, Air, and Soil Pollution.* 1, 50-64.

APPENDIX A

Cascade Impactor Particle Size Data

Table A-1 Atmospheric Metal Size Distribution at Kawishiwi Lab. (ng/m³)

Size Range (μm)	Fe	Al	Ca	Mn	Pb	Cu	Ni
>16	<22	93	ND*	0.62	<0.2	<0.7	<1.0
8-16	<22	24		0.37	<0.2	<0.7	<1.0
4-8	<22	23		0.46	<0.2	<0.7	<1.0
2-4	<22	17.0		<0.15	<0.2	1.4	<1.0
1-2	<22	7.5		<0.15	<0.2	<0.7	<1.0
.5-1	<22	7.5		<0.15	3.6	<0.7	<1.0
<.5	880	160		31	22	ND	<18
M _T	880	332		32.9	25.6	<4.9	<24
MMD (μm)	~.25	1.0		~.25	.27		
r ²		.94			1.00		
Impactor 1 Sampling Period: 9/8-9/76 Sample Volume: 13.62 m ³ Wind:							

* ND - Not Determined

Table A-2 Atmospheric Metal Size Distribution at Kawishiwi Lab. (ng/m³)

Size Range (μm)	Fe	Al	Ca	Mn	Pb	Cu	Ni
>16	24	37	ND*	0.62	0.37	2.8	<1.0
8-16	24	25		<0.15	<0.2	11.4	<1.0
4-8	<22	20		<0.15	<0.2	<0.7	<1.0
2-4	<22	16		<0.15	2.6	3.9	<1.0
1-2	78	37		<0.15	0.95	<0.7	<1.0
.5-1	<22	15		<0.15	0.37	<0.7	<1.0
<.5	<u>710</u>	<u>150</u>		<u><4</u>	<u>20</u>	<u>ND</u>	<u><18</u>
M _T	836	300		<5.4	24.69	20.2	<24
MMD (μm)	~.25	.59			.09		
r ²		.99			.91		
Impactor 2 Sampling Period: 9/8-9/76 Sample Volume: 13.62 m ³ Wind:							

* ND - Not Determined

Table A-3 Atmospheric Metal Size Distribution at Kawishiwi Lab. (ng/m³)

Size Range (μm)	Fe	Al	Ca	Mn	Pb	Cu	Ni
>16	<22	37	ND*	1.8	9.2	3.6	<1.0
8-16	<22	32		<0.15	1.7	10.3	<1.0
4-8	<22	22		<0.15	<.2	<0.7	<1.0
2-4	<22	21		<0.15	2.6	<0.7	<1.0
1-2	<22	11		0.32	3.2	2.8	<1.0
.5-1	<22	<5.0		0.16	2.1	1.9	6.9
<.5	850	150		82	<1	ND	<18
M _T	850	278		84.7	20.0	20.0	<31
MMD (μm)	~.25	.64		~.25	7.8	6.9	
r ²		.91			.90	.80	
Impactor 3	Sampling Period: 9/8-9/76		Sample Volume: 13.62 m ³		Wind:		

* ND - Not Determined

Table A-4 Atmospheric Metal Size Distribution at Kawishiwi Lab. (ng/m³)

Size Range (μm)	Fe	Al	Ca	Mn	Pb	Cu	Ni
>16	189	35	ND*	1.6	<0.2	<0.6	<1.0
8-16	183	28		2.2	0.35	<0.6	<1.0
4-8	208	35		2.4	1.4	<0.6	<1.0
2-4	102	9.4		1.2	<0.2	<0.6	<1.0
1-2	113	17		0.91	0.91	<0.6	<1.0
.5-1	47	13		0.91	0.79	<0.6	<1.0
<.5	654	110		25	<1.0	ND	<18
M _T	1496	247		34.2	4.85	<3.6	<24
MMD (μm)	1.2	1.1		.12	1.8		
r ²	.93	.93		.89	.97		
Impactor 1	Sampling Period: 9/23-24/76		Sample Volume: 16.5 m ³		Wind: NW		

* ND - Not Determined

Table A-5 Atmospheric Metal Size Distribution at Kawishiwi Lab. (ng/m³)

Size Range (μm)	Fe	Al	Ca	Mn	Pb	Cu	Ni
>16	213	35	ND*	1.7	1.7	0.6	1.0
8-16	235	34		1.7	0.67	1.4	1.0
4-8	136	16		1.7	0.2	0.6	1.0
2-4	163	22		1.7	1.6	1.9	1.0
1-2	80	12		1.0	1.5	0.6	1.0
.5-1	62	12		0.61	0.67	25	1.0
<.5	790	130		4	1	ND	18
M _T	1679	261		8.41	7.34	30.1	24
MMD (μm)	1.0	.76		5.8	3.2	.09	
r ²	.92	.93		1.00	.95	.94	
Impactor 2 Sampling Period: 9/23-24/76 Sample Volume: 16.5 m ³ Wind: NW							

* ND - Not Determined

Table A-6 Atmospheric Metal Size Distribution at Kawishiwi Lab. (ng/m³)

Size Range (μm)	Fe	Al	Ca	Mn	Pb	Cu	Ni
>16	188	78	ND*	1.9	1.2	<0.6	<1.0
8-16	143	53		1.9	2.1	13.3	<1.0
4-8	173	46		2.0	0.42	<0.6	<1.0
2-4	84	20		1.3	<0.2	<0.6	<1.0
1-2	125	24		0.91	1.8	<0.6	<1.0
.5-1	20	29		0.91	1.5	0.9	<1.0
<.5	680	170		25	<1	ND	<18
M _T	1413	420		33.92	8.22	16.6	<24
MMD (μm)	.95	1.4		.08	3.0	6.3	
r ²	.94	.95		.92	.92	.67	
Impactor 3 Sampling Period: 9/23-24/76 Sample Volume: 16.5 m ³ Wind: NW							

* ND - Not Determined

Table A-7 Atmospheric Metal Size Distribution at Kawishiwi Lab. (ng/m³)

Size Range (μm)	Fe	Al	Ca	Mn	Pb	Cu	Ni
>16	949	1289	ND*	19.8	8.9	ND	20.7
8-16	860	589		9.9	15.2		62.0
4-8	1702	485		13.8	57.8		660
2-4	293	271		5.0	9.3		124
1-2	773	251		8.6	47.8		282
.5-1	1866	298		13.3	94.6		63.2
<.5	606	120		<4	<1		<17
M _T	7049	3303		74.4	235		1212
MMD (μm)	2.9	9.8		4.9	2.6		3.5
r ²	.94	.98		.95	.84		.96
Impactor 3 Sampling Period: 11/18-19/76 Sample Volume: 17.15 m ³ Wind: NW - 10-15							

* ND - Not Determined

Table A-8 Atmospheric Metal Size Distribution at Kawishiwi Lab. (ng/m³)

Size Range (μm)	Fe	Al	Ca	Mn	Pb	Cu	Ni
>16	140	11	ND*	2.0	1.4	8.2	<1.0
8-16	141	8.0		1.8	1.7	13.8	<1.0
4-8	78	11		1.5	2.0	0.8	<1.0
2-4	70	6.4		1.4	1.8	<0.4	<1.0
1-2	90	6.8		0.82	2.6	1.2	<1.0
.5-1	139	22		0.56	3.2	1.0	<1.0
<.5	180	48		<6	6.5	ND	<11
M _T	838	113		8.08	19.2	25.4	<17
MMD (μm)	2.4	.69		6.9	1.1	12.3	
r ²	.98	.97		1.00	1.00	.75	
Impactor 1 Sampling Period: 2/18-20/77 Sample Volume: 27.6 m ³ Wind: NW 0-10							

* ND - Not Determined

Table A-9 Atmospheric Metal Size Distribution at Kawishiwi Lab. (ng/m³)

Size Range (μm)	Fe	Al	Ca	Mn	Pb	Cu	Ni
>16	101	11	ND*	<0.07	1.3	2.3	<1.0
8-16	49	8.0		<0.07	1.3	1.6	<1.0
4-8	62	6.2		0.11	1.3	1.3	<1.0
2-4	36	6.2		0.23	1.4	1.2	<1.0
1-2	40	6.8		0.43	2.4	<0.4	<1.0
.5-1	23	8.1		0.73	2.5	1.0	<1.0
<.5	180	34		26	<1	ND	18
M _T	491	80		27.6	11.2	7.8	<24
MMD (μm)	1.8	.88		~.25	2.5	7.5	
r ²	.97	.99		.97	.96	.98	
Impactor 3 Sampling Period: 2/18-20/77 Sample Volume: 27.6 m ³ Wind: NW 0-10							

* ND - Not Determined

Table A-10 Atmospheric Metal Size Distribution at Kawishiwi Lab. (ng/m³)

Size Range (μm)	Fe	Al	Ca	Mn	Pb	Cu	Ni
>16	760	173	ND*	3.8	2.8	3.8	<1.0
8-16	443	92		3.2	4.0	88	<1.0
4-8	266	157		2.8	4.1	11	<1.0
2-4	205	78		2.4	3.3	2.0	<1.0
1-2	120	56		1.7	3.1	2.5	<1.0
.5-1	60	90		1.0	2.8	2.1	<1.0
<.5	120	58		<2	<1	ND	<14
M _T	1974	704		14.9	21.1	109	<20
MMD (μm)	11.7	5.0		6.9	3.9	1.14	
r ²	.98	.99		1.00	.99	.74	
Impactor 2 Sampling Period: 3/22-23/77 Sample Volume: 21.32 m ³ Wind: W 5-15							

* ND - Not Determined

Table A-11 Atmospheric Metal Size Distribution at Kawishiwi Lab. (ng/m³)

Size Range (μm)	Fe	Al	Ca	Mn	Pb	Cu	Ni
>16	799	167	ND*	3.7	1.5	<0.5	<1.0
8-16	448	110		3.3	4.4	2.0	<1.0
4-8	351	94		3.0	3.4	<0.5	<1.0
2-4	144	59		1.9	2.4	<0.5	<1.0
1-2	114	69		1.5	3.4	1.1	3.6
.5-1	40	44		0.8	3.1	<0.5	1.2
<.5	200	58		<2	2.8	ND	<14
M _T	2096	601		14.2	21.0	<5.1	<22.8
MMD (μm)	11.5	6.1		7.4	2.6		
r ²	.94	.99		1.00	.98		
Impactor 3	Sampling Period: 3/22-23/77		Sample Volume: 21.32 m ³		Wind: W 5-15		

* ND - Not Determined

Table A-12 Atmospheric Metal Size Distribution at Kawishiwi Lab. (ng/m³)

Size Range (μm)	Fe	Al	Ca	Mn	Pb	Cu	Ni	Cd	Co	Zn
>16	52	64	75	1.22	0.72	<0.1	1.2	0.024	<.2	1.4
8-16	48	47	69	0.56	0.64	<0.1	<0.3	0.016	<.2	.5
4-8	54	33	58	0.60	1.2	<0.1	<0.3	0.006	<.2	.5
2-4	76	47	48	0.90	2.0	<0.1	1.4	0.013	<.2	.9
1-2	26	23	8.7	0.30	2.7	<0.1	<0.3	0.012	<.2	1.1
.5-1	6.7	10	3.8	0.40	7.6	<0.1	<0.3	0.050	<.2	1.7
<.5	28	15	10	<.5	2.8	ND*	<3	ND	<.2	ND
M _T	291	239	273	4.05	17.7	<0.6	<6.8	.12	<1.4	6.1
MMD (μm)	4.6	6.5	8.4	6.6	1.2			1.89		2.87
r ²	.97	.99	.95	.99	.91			.98		.97
Impactor 3 Sampling Period: 5/21-27/77 Sample Volume: 107.81 m ³ Wind: SE 5-15+										

* ND - Not Determined

Table A-13 Atmospheric Metal Size Distribution at Kawishiwi Lab. (ng/m³)

Size Range (μm)	Fe	Al	Ca	Mn	Pb	Cu	Ni
>16	240	285	96	2.6	0.8	0.8	<1
8-16	180	180	90	2.3	1.4	14	<1
4-8	158	195	105	2.3	3.2	3.2	<1
2-4	120	120	43	0.7	2.8	1.4	<1
1-2	68	58	26	1.1	4.1	7.0	<1
.5-1	62	50	18	1.0	5.6	9.0	2.5
<.5	<14	44	33	<0.8	35	ND*	<5
M _T	828	932	411	10.0	52.9	35.4	<12.5
MMD (μm)	7.5	8.1	6.5	7.3	.20	3.1	
r ²	.99	.99	.95	.98	1.00	.80	
Impactor 3	Sampling Period: 7/25-29/77		Sample Volume: 72.0 m ³		Wind: N 5-10		

* ND - Not Determined

Table A-14 Atmospheric Metal Size Distribution at Kawishiwi Lab. (ng/m³)

Size Range (μm)	Fe	Al	Ca	Mn	Pb	Cu	Ni
>16	215	170	44	1.9	0.4	2.0	2.4
8-16	14	110	32	0.9	<0.3	<0.3	<1.5
4-8	<3	21	11	0.4	<0.3	1.5	<1.5
2-4	3.5	80	10	0.4	0.4	<0.3	<1.5
1-2	<3	95	<4	<0.1	<0.3	<0.3	<1.5
.5-1	3.5	83	<4	<0.1	<0.3	<0.3	<1.5
<.5	<25	16	<10	<3	2.5	ND*	3.1
M _T	236	575	97	3.8	3.3	4.70	<13.0
MMD (μm)	>16	5.5	14.9	17.2	.04		
r ²		.92	.97	.99	.77		
Impactor 2	Sampling Period: 9/9-11/77		Sample Volume: 40.5 m ³		Wind: W-NW 5-10		

* ND - Not Determined

Table A-15 Atmospheric Metal Size Distribution at Kawishiwi Lab. (ng/m³)

Size Range (μm)	Fe	Al	Ca	Mn	Pb	Cu	Ni
>16	130	100	44	0.8	<0.1	<0.2	<1
8-16	9.2	67	19	0.8	<0.1	0.3	<1
4-8	7.2	55	33	0.8	0.3	0.3	<1
2-4	9.6	29	20	0.9	0.6	0.4	<1
1-2	8.7	37	12	0.4	0.7	0.3	<1
.5-1	18	63	<3	0.5	1.1	0.4	<1
<.5	<17	70	26	<1.0	<1.0	ND*	<5
M _T	183	421	157	4.2	3.7	1.7	<11.0
MMD (μm)	>16	3.9	5.5	5.2	.92	2.5	
r ²		.98	.96	1.00	.99	1.00	
Impactor 2 Sampling Period: 10/9-13/77 Sample Volume: 57.6 m ³ Wind: W-NW 5-10							

* ND - Not Determined

Table A-16 Atmospheric Metal Size Distribution at Kawishiwi Lab. (ng/m³)

Size Range (μm)	Fe	Al	Ca	Mn	Pb	Cu	Ni
>16	6.6	110	14	1.3	<0.1	<0.1	<0.8
8-16	9.3	43	87	1.3	0.3	<0.1	<0.8
4-8	10	40	80	2.1	1.7	<0.1	<0.8
2-4	7.4	41	2	1.7	2.0	<0.1	<0.8
1-2	2.6	35	< 2	0.9	3.0	<0.1	<0.8
.5-1	3.9	26	<2	0.9	4.2	<0.1	<0.8
<.5	<13	16	<7	10	28	ND*	<4
M _T	39.8	311	194	18.2	39.3	<0.60	<8.8
MMD (μm)	5.7	7.5	6.1	.56	.17		
r ²	.98	.99	.76	.95	.99		
Impactor 2 Sampling Period: 11/13-17/77 Sample Volume: 76.1 m ³ Wind: SE 5-10							

* ND - Not Determined

Table A-17 Atmospheric Metal Size Distribution at Kawishiwi Lab. (ng/m³)

Size Range (μm)	Fe	Al	Ca	Mn	Pb	Cu	Ni
>16	5.1	22	5	1.0	<0.1	<0.1	<0.7
8-16	6.9	25	5	0.9	0.1	<0.1	<0.7
4-8	<2	24	4	1.1	0.2	<0.1	<0.7
2-4	3.1	16	4	1.1	0.2	<0.1	<0.7
1-2	<2	51	4	1.0	0.2	<0.1	<0.7
.5-1	6.4	14	2	1.1	0.5	<0.1	<0.7
<.5	<11	2.3	<5	11	2.7	ND*	<3
M _T	21.5	154	24.0	17.2	4.0	<0.6	<7.2
MMD (μm)	4.5	4.0	5.6	.21	.14		
r ²	.93	.95	.99	.99	.99		
Impactor 2	Sampling Period: 11/17-22/77		Sample Volume: 90.1 m ³		Wind: NW <5		

* ND - Not Determined

Table A-18 Atmospheric Metal Size Distribution at Hoyt Lakes (ng/m³)

Size Range (μm)	Fe	Al	Ca	Mn	Pb	Cu	Ni
>16	1438	1135	ND*	24	3.1	ND	<1.0
8-16	1071	788		14	4.2		<1.0
4-8	892	614		16	6.7		<1.0
2-4	417	309		7.5	3.0		<1.0
1-2	238	191		5.4	3.9		<1.0
.5-1	102	91		2.6	3.2		<1.0
<.5	770	360		2.6	<1		<16
M _T	4928	3488		95	25		<22
MMD (μm)	7.1	8.9		3.9	4.0		
r ²	.91	.94		.93	.99		
Impactor 2 Sampling Period: 11/18-19/76 Sample Volume: 18.42 m ³ Wind: NW 10-15							

* ND - Not Determined

Table A-19 Atmospheric Metal Size Distribution at Hoyt Lakes (ng/m³)

Size Range (μm)	Fe	Al	Ca	Mn	Pb	Cu	Ni
>16	980	766	ND*	20.1	2.3	1.1	<1.0
8-16	815	576		21.4	3.0	0.9	<1.0
4-8	645	388		14.9	3.0	2.3	<1.0
2-4	408	337		10.5	2.7	0.6	<1.0
1-2	261	201		4.9	3.9	5.4	<1.0
.5-1	162	96		3.1	2.7	2.3	<1.0
<.5	760	210		23	6	ND	59
M _T	4031	2586		97.9	23.6	12.6	65
MMD (μm)	5.0	7.8		4.0	1.8	2.4	
r ²	.94	.98		.98	.99	.91	

Impactor 2 Sampling Period: 11/18-19/76 Sample Volume: 18.42 m³ Wind: NW 10-15

* ND - Not Determined

Table A-20 Atmospheric Metal Size Distribution at Hoyt Lakes (ng/m³)

Size Range (μm)	Fe	Al	Ca	Mn	Pb	Cu	Ni
>16	1682	19	ND*	<.07	1.3	2.7	<1.0
8-16	844	20		0.10	2.1	8.9	<1.0
4-8	621	19		0.10	2.4	3.0	<1.0
2-4	444	18		0.72	3.5	4.9	<1.0
1-2	277	12		0.54	3.5	14.0	<1.0
.5-1	105	5.7		0.65	3.4	3.1	<1.0
<.5	340	60		160	18	ND	<10
M _T	4313	154		162	34.2	36.6	<16
MMD (μm)	10.3	1.5		~.25	.49	3.5	
r ²	.97	.95			.99	.92	
Impactor 2 Sampling Period: 2/18-20/77 Sample Volume: 30.32 m ³ Wind: NW 0-10							

* ND - Not Determined

Table A-21 Atmospheric Metal Size Distribution at Hoyt Lakes (ng/m³)

Size Range (μm)	Fe	Al	Ca	Mn	Pb	Cu	Ni
>16	203	36	ND*	0.75	1.2	<0.6	<1.0
8-16	160	32		0.54	1.2	0.7	<1.0
4-8	56	42		0.62	2.0	<0.6	<1.0
2-4	37	33		0.39	2.2	<0.6	<1.0
1-2	32	24		0.29	2.0	<0.6	<1.0
.5-1	<13	10		0.18	2.5	<0.6	<1.0
<.5	80	34		<2	<1	ND	<12
M _T	568	211		2.77	12.1	<3.7	<18
MMD (μm)	10.2	3.7		7.3	2.6		
r ²	.99	.98		1.00	.99		
Impactor 1	Sampling Period: 3/22-23/77		Sample Volume: 24.06 m ³		Wind: W 5-10		

* ND - Not Determined

Table A-22 Atmospheric Metal Size Distribution at Hoyt Lakes (ng/m³)

Size Range (μm)	Fe	Al	Ca	Mn	Pb	Cu	Ni
>16	330	180	39	7.9	2.2	1.9	7.6
8-16	220	99	40	2.9	1.1	1.1	<2.5
4-8	290	150	58	4.3	1.6	1.1	<2.5
2-4	300	220	26	2.9	1.2	<0.4	<2.5
1-2	110	60	180	2.1	1.6	<0.4	<2.5
.5-1	460	64	41	2.3	5.8	6.6	<2.5
<.5	54	17	22	<2	5.0	ND	<11
M _T	1764	790	406	22.4	18.5	10.7	<31.1
MMD (μm)	3.8	5.5	2.7	8.1	1.1	.73	
r ²	.92	.99	.94	1.00	.92	.77	
Impactor 2 Sampling Period: 7/25-26/77 Sample Volume: 25.8 m ³ Wind: N 5-10							

* ND - Not Determined

Table A-23 Atmospheric Metal Size Distribution at Hoyt Lakes (ng/m³)

Size Range (μm)	Fe	Al	Ca	Mn	Pb	Cu	Ni
>16	27	73	36	1.7	0.2	4.3	2.4
8-16	7.2	44	15	1.1	0.2	0.2	1.5
4-8	8.0	30	16	0.8	0.7	0.2	1.5
2-4	9.5	55	19	0.8	0.3	0.3	1.5
1-2	5.8	63	19	0.5	1.0	0.2	1.5
.5-1	5.2	15	13	0.6	2.9	0.2	1.5
<.5	19	46	10	3	3.5	ND*	3.1
M _T	63	326	118	5.5	8.6	5.4	13
MMD (μm)	10.3	3.9	6.1	8.0	.52		
r ²	.99	.98	.98	1.00	.92		
Impactor 3 Sampling Period: 9/8-11/77 Sample Volume: 51.6 m ³ Wind: W-NW 5-10							

* ND - Not Determined

Table A-24 Atmospheric Metal Size Distribution at Hoyt Lakes (ng/m³)

Size Range (μm)	Fe	Al	Ca	Mn	Pb	Cu	Ni
>16	270	120	68	5.5	0.3	<0.5	<2.7
8-16	350	410	79	4.9	0.9	3.4	7.4
4-8	230	300	80	3.6	2.0	<0.5	3.4
2-4	49	100	63	3.6	2.6	0.7	<2.7
1-2	17	230	<7	2.0	4.0	<0.5	<2.7
.5-1	32	110	13	1.8	9.4	1.5	<2.7
<.5	190	38	<20	<2	36	ND*	<13
M _T	1138	1308	303	21.4	55.2	5.6	<34.6
MMD (μm)	6.4	4.6	7.7	7.0	.19	4.4	
r ²	.80	.97	.95	1.00	.99	.78	
Impactor 1 Sampling Period: 10/9-13/77 Sample Volume: 22.4 m ³ Wind: W-NW 5-10							

* ND - Not Determined

Table A-25 Atmospheric Metal Size Distribution at Hoyt Lakes (ng/m³)

Size Range (μm)	Fe	Al	Ca	Mn	Pb	Cu	Ni
>16	28	61	112	1.1	2.1	0.3	<0.8
8-16	20	86	204	1.3	2.4	0.3	<0.8
4-8	24	69	192	1.5	5.7	0.4	<0.8
2-4	15	41	101	1.1	5.9	0.5	<0.8
1-2	10	39	84	0.9	6.3	0.6	<0.8
.5-1	4	25	59	0.8	11	0.6	<0.8
<.5	<13	16	<7	<0.6	40	ND*	<4
M _T	101	337	759	7.3	73.4	3.3	<8.8
MMD (μm)	7.7	5.5	5.6	5.6	.38	1.9	
r ²	1.00	.99	.98	.86	1.00	.99	
Impactor 1	Sampling Period: 11/13-17/77		Sample Volume: 75.8 m ³		Wind: SE 5-10		

* ND - Not Determined

Table A-26 Atmospheric Metal Size Distribution at Hoyt Lakes (ng/m³)

Size Range (μm)	Fe	Al	Ca	Mn	Pb	Cu	Ni
>16	22	44	11	1.3	<0.1	<0.1	<0.7
8-16	15	79	9	1.1	0.1	<0.1	<0.7
4-8	9.6	23	7	1.1	0.7	<0.1	<0.7
2-4	5.8	29	4	1.0	0.4	<0.1	<0.7
1-2	9.0	25	2	1.6	0.9	<0.1	<0.7
.5-1	3.0	93	<2	1.0	0.8	<0.1	<0.7
<.5	18	13	12	18	7.3	ND*	<3
M _T	82.4	306	47	25.1	10.3	<0.6	<7.2
MMD (μm)	4.6	3.5	4.0	.08	.18		
r ²	.96	.88	.91	.99	.98		
Impactor 1 Sampling Period: 11/17-22/77 Sample Volume: 90.5 m ³ Wind: NW <5							

* ND - Not Determined

Table A-27 Atmospheric Metal Size Distribution at Univ. of Minn. (ng/m³)

Size Range (μm)	Fe	Al	Ca	Mn	Pb	Cu	Ni
>16	920	1010	750	10	73	<.5	<3
8-16	830	830	650	10	84	2.4	<3
4-8	990	790	670	12	150	3.8	<3
2-4	640	1010	260	5.4	110	1.5	<3
1-2	460	470	240	8.1	120	1.6	<3
.5-1	380	640	340	34	200	3.8	<3
<.5	340	150	150	60	1040	ND*	<16
M _T	4560	4900	3060	139.5	1777	13.7	<34
MMD (μm)	5.0	4.9	6.2	.58	.32	3.2	
r ²	.99	.98	.98	.95	.99	.92	
Impactor 1 Sampling Period: 2/15-16/77 Sample Volume: 18.6 m ³ Wind: NW 6 mph							

* ND - Not Determined

Table A-28 Atmospheric Metal Size Distribution at Univ. of Minn. (ng/m³)

Size Range (μm)	Fe	Al	Ca	Mn	Pb	Cu	Ni
>16	940	980	710	12	68	7.5	114
8-16	1610	970	1400	7.5	100	2.5	<3
4-8	840	830	610	7.5	100	11	<3
2-4	600	580	330	7.0	130	2.7	<3
1-2	740	650	320	6.5	120	2.1	<3
.5-1	410	330	170	20	140	2.3	<3
<.5	330	200	44	66	790	ND*	<16
M _T	5470	4540	3584	126.5	1448	28.1	145
MMD (μm)	5.3	5.6	7.5	.35	.44	6.7	
r ²	.98	1.00	.97	.98	.99	.95	
Impactor 2 Sampling Period: 2/15-16/77 Sample Volume: 18.6 m ³ Wind: NW 6 mph							

* ND - Not Determined

APPENDIX B

Mass Median Diameter Calculation

For an aerosol distribution, mass median diameter is defined as the particle diameter, usually reported in μm , at which half of the aerosol mass is found on particles of diameter greater than the mmd and half on particles less than the mmd. Mass median diameters were calculated with the aid of a Hewlett-Packard (HP-97) desk-top calculator utilizing the program on the following page. The program was developed by combining and modifying linear regression and inverse normal integral programs supplied with the HP-25 hand calculator. To calculate mmd, the number of stages is input into the HP-97 calculator, followed by the metal concentration of each stage, beginning with the back-up filter. The fraction of mass below each size cut-off is calculated and converted to probability units; both are printed out. The probability units and corresponding size cut-off (log diameter) are input into the calculator in pairs until all stages have been entered. The points will be fit to a line by linear regression analysis, and the slope, correlation coefficient (r^2), and mmd will be printed out. A sample calculation is shown on page B-4.

Program for Calculating mmd

B-3

001	*LELA	048	RCL4	095	0	142	R4
002	ST00	049	BSBC	096	+	143	X#Y
003	X#I	050	RCL5	097	x	144	Z#
004	RTH	051	BSBC	098	1	145	RTH
005	*LELA	052	RCL5	099	+	146	*LELE
006	ST01	053	BSBC	100	ST0A	147	FFB
007	BSBE	054	RCL7	101	CLX	148	RCL3
008	RTH	055	BSBC	102	.	149	RCL4
009	*LELA	056	*LELC	103	0	150	RCL5
010	ST02	057	ST+B	104	1	151	x
011	BSBE	058	RCL5	105	0	152	RCL5
012	RTH	059	RCL6	106	3	153	=
013	*LELA	060	.	107	2	154	-
014	ST03	061	FRTX	108	8	155	RCL5
015	BSBE	062	ENT1	109	x	156	RCL4
016	RTH	063	x	110	.	157	X#
017	*LELA	064	1/X	111	6	158	RCL5
018	ST04	065	LN	112	0	159	=
019	BSBE	066	JN	113	2	160	-
020	RTH	067	ST05	114	6	161	=
021	*LELA	068	ENT1	115	5	162	ST0E
022	ST05	069	ENT1	116	3	163	RCL4
023	BSBE	070	ENT1	117	+	164	x
024	RTH	071	.	118	x	165	CH3
025	*LELA	072	0	119	2	166	RCL5
026	ST06	073	0	120	.	167	+
027	BSBE	074	1	121	5	168	RCL5
028	RTH	075	3	122	1	169	=
029	*LELA	076	0	123	5	170	ST0C
030	ST07	077	8	124	5	171	RCL5
031	BSBE	078	x	125	1	172	FRTX
032	*LELE	079	.	126	7	173	X#Y
033	ST+B	080	1	127	+	174	R4
034	DSZ1	081	6	128	RCL4	175	x
035	RTH	082	9	129	=	176	RCL7
036	RCL3	083	2	130	-	177	RCL5
037	SFC	084	5	131	CH3	178	X#
038	FRTX	085	3	132	FRTX	179	RCL5
039	SFC	086	+	133	SFC	180	=
040	RCL6	087	x	134	DSZ1	181	-
041	X#I	088	1	135	RTH	182	=
042	RCL1	089	.	136	CLAG	183	FRTX
043	BSBC	090	4	137	FAS	184	RCL5
044	RCL5	091	3	138	RAS	185	FRTX
045	BSBC	092	2	139	*LELE	186	RTH
046	RCL3	093	7	140	ENT1	187	RAS
047	BSBC	094	5	141	Z#		

Sample Run of MMD Program

Input:	No. of Stages → 7.00 G55A 58.00 G55A 66.00 G55A 77.00 G55A Mass in each Stage → 150.00 G55A 200.00 G55A 240.00 G55A 300.00 G55A
Output:	Total Mass → 1241.00 *** Fraction under Stage 1 → 0.05 *** -1.20 *** Probability (Std. Dev. Units) → 0.10 *** -1.20 *** 0.10 *** -0.95 *** 0.20 *** -0.55 *** 0.50 *** 1.007016000-05 *** 0.60 *** 0.50 *** 1.00 *** 2.52 *** Probability (Std. Dev. Units) → -1.60 ENT? -1.301 G55D -1.20 ENT? 0.80 G55D log of cut-off size → -0.99 ENT? .301 G55D -.55 ENT? .582 G55D 1.007-05 ENT? .305 G55D .50 ENT? 1.204 G55D G55E Slope → 0.65 *** Correlation coef. (r ²) → 0.55 ** log MMD → 0.51 *** 10 ⁴ (MMD(μm)) → 0.11 ***

APPENDIX C

Calculation of Loading Rates
Due to Dry Deposition

Deposition velocities can be obtained using the data from Figure C-1 from Sehmel and Sutter, (1974). For this report, loading rates were calculated for each stage, then the rates were summed to obtain total loading. First it was necessary to assign a diameter to each size range in order to make use of Figure C-1. It was decided to use the geometric mean of the upper and lower cut-offs of each stage as the characteristic diameter. A second problem was the assignment of an upper cut-off for stage 1 and a lower cut-off for the back-up filter. Since stages 2 through 6 are of equal geometric intervals, the same was assumed true for stage 1, yielding an upper boundary of 32 μm . For the back-up filter, .08 μm was used as the lower cut-off as this is the approximate lower boundary of the accumulation mode of a bimodal distribution.

Since the size ranges are relatively broad for cascade impactors, some error may result from using only one value of particle diameter for each stage. However, any attempt to further breakdown the concentrations with respect to size would be speculative at best and may result in a greater error in final loading rate.

In order to use the data in Figure C-1, one additional correction is necessary. Sehmel and Sutter (1974) used spherical particles of density equal to 1.5 g/cm^3 . Aerosols in this study were collected on the basis of aerodynamic diameter, which assumes spherical shape of unit density. As a result, a particle of a given diameter from Sehmel and Sutter's work would have a greater terminal settling velocity than a particle with the same diameter as collected by the cascade impactor. For particles of equal settling velocities the following relationship can be derived:

$$d_p^2 P_p C_p = d_a^2 P_a C_a$$

where d_p and d_a are the actual diameter and the aerodynamic diameter, respectively; P_p is the particle density and P_a is the aerodynamic particle density, equal to

1.0 by definition. C_p and C_a are slip correction factors and can be assumed to be approximately equal. From the above relationship, aerodynamic diameters can be converted to diameters equivalent to particles of 1.5 g/cm^3 density as follows:

$$d = \sqrt{d_a^2 / 1.5}$$

After correction of the particle diameter, the deposition velocity V_g can be determined from Figure C-1. The loading rate for each stage is then calculated:

$$\text{Loading rate } (\phi) = V_g \cdot X$$

where X is the concentration of the metal in the stage corresponding to the particle diameter d above. If X is in units of ng/m^3 and V_g is in units of m/sec , ϕ will be in $\text{ng/m}^3\text{-sec}$. This can be converted to kg/ha-yr by multiplication by a conversion factor of 0.315.

The above procedure is carried out for all seven stages and the resulting rates are summed to obtain a total loading rate.

Figure C-1.
Deposition velocities to a water surface (particle density of 1.5 g/cm^3).
(From Schmel and Sutter, 1974).

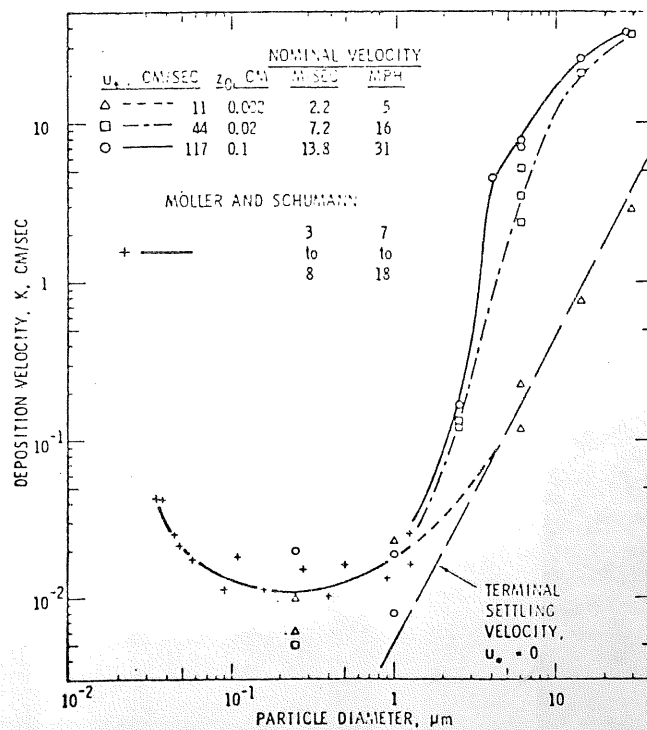


Figure C-1. Deposition velocities to a water surface (particle density of 1.5 g/cm^3). (From Sehmel and Sutter, 1974).